Prepared in cooperation with the Iowa Department of Transportation and the Iowa Highway Research Board (Project TR–692)

Stream-Channel and Watershed Delineations and Basin-Characteristic Measurements using Lidar Elevation Data for Small Drainage Basins within the Des Moines Lobe Landform Region in Iowa

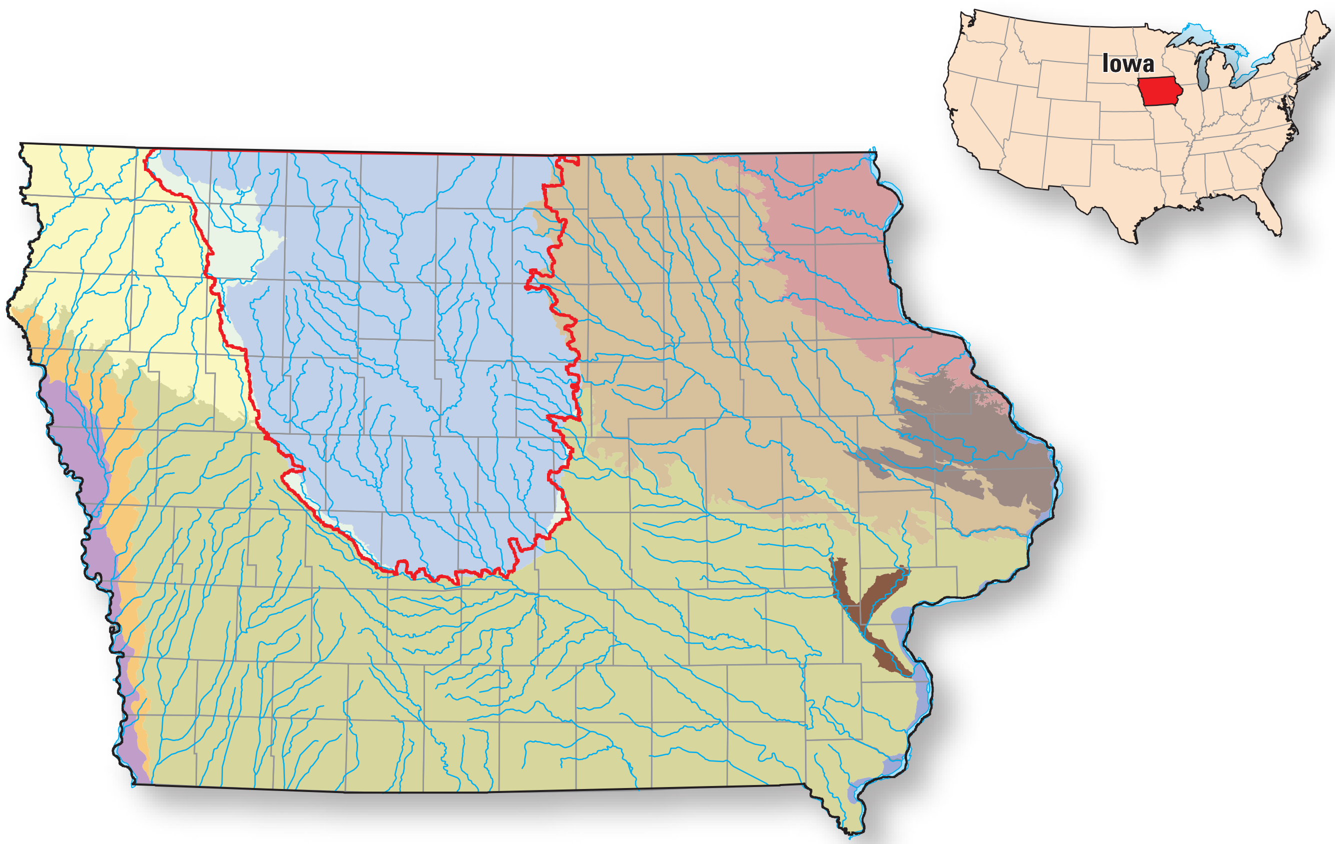

Scientific Investigations Report 2017–5108

U.S. Department of the Interior
U.S. Geological Survey

Stream-Channel and Watershed Delineations and Basin-Characteristic Measurements using Lidar Elevation Data for Small Drainage Basins within the Des Moines Lobe Landform Region in Iowa

By David A. Eash, Kimberlee K. Barnes, Padraic S. O'Shea, and Brian K. Gelder

Prepared in cooperation with the Iowa Department of Transportation and the Iowa Highway Research Board (Project TR–692)

Scientific Investigations Report 2017–5108

U.S. Department of the Interior
U.S. Geological Survey

U.S. Department of the Interior
RYAN K. ZINKE, Secretary

U.S. Geological Survey
William H. Werkheiser, Deputy Director
exercising the authority of the Director

U.S. Geological Survey, Reston, Virginia: 2018

For more information on the USGS—the Federal source for science about the Earth, its natural and living resources, natural hazards, and the environment—visit https://www.usgs.gov or call 1–888–ASK–USGS.

For an overview of USGS information products, including maps, imagery, and publications, visit https://store.usgs.gov.

Suggested citation:
Eash, D.A., Barnes, K.K., O'Shea, P.S., and Gelder, B.K., 2018, Stream-channel and watershed delineations and basin-characteristic measurements using lidar elevation data for small drainage basins within the Des Moines Lobe landform region in Iowa: U.S. Geological Survey Scientific Investigations Report 2017–5108, 23 p., https://doi.org/10.3133/sir20175108.

ISSN 2328-0328 (online)

Contents

Figures

Tables

Conversion Factors

U.S. customary units to International System of Units

Multiply	By	To obtain
	Length	
inch (in.)	2.54	centimeter (cm)
foot (ft)	0.3048	meter (m)
mile (mi)	1.609	kilometer (km)
foot per mile (ft/mi)	0.1894	meter per kilometer (m/km)
	Area	
square mile (mi^2)	2.590	square meter (m^2)
square feet (ft^2)	0.09290	square meter (m^2)
mile per square mile ($mi^{2/mi}$)	0.621	kilometer per square kilometer (km/km^2)
square mile per mile ($mi^{2/mi}$)	1.609	square kilometer per kilometer (km^2/km)
	Flow rate	
cubic foot per second (ft^3/s)	0.02832	cubic meter per second (m^3/s)

International System of Units to U.S. customary units

Multiply	By	To obtain
	Length	
meter (m)	3.281	foot (ft)
	Area	
Square meter (m^2)	10.7	square feet (ft^2)

Datum

Vertical coordinate information is referenced to the North American Vertical Datum of 1988 (NAVD 88).

Horizontal coordinate information is referenced to the North American Datum of 1983 (NAD 83).

Map projections are Universal Transverse Mercator, Zone 15 North.

Supplemental Information

Water year is the 12-month period from October 1 through September 30. The water year is designated by the calendar year in which the water year ends and includes 9 of the 12 months of that year. Thus, the water year ending September 30, 2015, is the "2015 water year."

Abbreviations

AEP	annual exceedance probability
AEPD	annual exceedance-probability discharge
CCM	constant of channel maintenance
CON	continuous streamgage
DEM	digital elevation model
DOT	department of transportation
DRNAREA	geographic information system-determined drainage area
DRNFREQ	drainage frequency
EMA/MGB	expected moments algorithm annual exceedance-probability analysis with Multiple Grubbs-Beck low-outlier test
FOSTREAM	number of first-order streams
GIS	geographic information system
GLS	generalized least-squares
GPS	global positioning system
HUC	hydrologic unit code
IDNR	Iowa Department of Natural Resources
IIHR	Iowa Institute of Hydraulic Research
lidar	light detection and ranging
MGB	Multiple Grubbs-Beck low-outlier test
NHD	National Hydrography Dataset
Pseudo-R^2	pseudo coefficient of determination
$Q_{50\%}$	annual exceedance-probability discharge of 50 percent (2-year recurrence-interval flood discharge)
$Q_{20\%}$	annual exceedance-probability discharge of 20 percent (5-year recurrence-interval flood discharge)
$Q_{10\%}$	annual exceedance-probability discharge of 10 percent (10-year recurrence-interval flood discharge)
$Q_{4\%}$	annual exceedance-probability discharge of 4 percent (25-year recurrence-interval flood discharge)
$Q_{2\%}$	annual exceedance-probability discharge of 2 percent (50-year recurrence-interval flood discharge)
$Q_{1\%}$	annual exceedance-probability discharge of 1 percent (100-year recurrence-interval flood discharge)
$Q_{0.5\%}$	annual exceedance-probability discharge of 0.5 percent (200-year recurrence-interval flood discharge)
$Q_{0.2\%}$	annual exceedance-probability discharge of 0.2 percent (500-year recurrence-interval flood discharge)
RRE	regional regression equation
RSD	relative stream density
SEM	standard error of model
SEP	average standard error of prediction
StreamStats	U.S. Geological Survey web-based geographic information system tool (http://water.usgs.gov/osw/streamstats/index.html)
STRDEN	stream density
STRMTOT	total length of all mapped streams in a basin
SSURGO	National Resources Conservation Service Soil Survey Geographic database
USGS	U.S. Geological Survey
WBD	Watershed Boundary Dataset

Stream-Channel and Watershed Delineations and Basin-Characteristic Measurements using Lidar Elevation Data for Small Drainage Basins within the Des Moines Lobe Landform Region in Iowa

By David A. Eash[1], Kimberlee K. Barnes[1], Padraic S. O'Shea[1], and Brian K. Gelder[2]

Abstract

Basin-characteristic measurements related to stream length, stream slope, stream density, and stream order have been identified as significant variables for estimation of flood, flow-duration, and low-flow discharges in Iowa. The placement of channel initiation points, however, has always been a matter of individual interpretation, leading to differences in stream definitions between analysts.

This study investigated five different methods to define stream initiation using 3-meter light detection and ranging (lidar) digital elevation models (DEMs) data for 17 streamgages with drainage areas less than 50 square miles within the Des Moines Lobe landform region in north-central Iowa. Each DEM was hydrologically enforced and the five stream initiation methods were used to define channel initiation points and the downstream flow paths. The five different methods to define stream initiation were tested side-by-side for three watershed delineations: (1) the total drainage-area delineation, (2) an effective drainage-area delineation of basins based on a 2-percent annual exceedance probability (AEP) 12-hour rainfall, and (3) an effective drainage-area delineation based on a 20-percent AEP 12-hour rainfall.

Generalized least squares regression analysis was used to develop a set of equations for sites in the Des Moines Lobe landform region for estimating discharges for ungaged stream sites with 50-, 20-, 10-, 4-, 2-, 1-, 0.5-, and 0.2-percent AEPs. A total of 17 streamgages were included in the development of the regression equations. In addition, geographic information system software was used to measure 58 selected basin-characteristics for each streamgage.

Results of the regression analyses of the 15 lidar datasets indicate that the datasets that produce regional regression equations (RREs) with the best overall predictive accuracy are the National Hydrographic Dataset, Iowa Department of Natural Resources, and profile curvature of 0.5 stream initiation methods combined with the 20-percent AEP 12-hour rainfall watershed delineation method. These RREs have a mean average standard error of prediction (SEP) for 4-, 2-, and 1-percent AEP discharges of 53.9 percent and a mean SEP for all eight AEPs of 55.5 percent. Compared to the RREs developed in this study using the basin characteristics from the U.S. Geological Survey StreamStats application, the lidar basin characteristics provide better overall predictive accuracy.

Introduction

Because light detection and ranging (lidar) elevation data are available for Iowa (www.iowagic.org/projects/lidar-for-iowa/) and an automated process for enforcing drainage networks on 3-meter (m) lidar digital elevation models (DEMs) has been developed (Gelder, 2015), accurate drainage networks can be delineated for the appropriate hydrologic enforcement of lidar DEMs and measurement of drainage-basin characteristics. Lidar refers to the process of scanning the earth with lasers from an aircraft to obtain accurate elevations (https://www.legis.iowa.gov/docs/publications/SD/4767.pdf). The lidar instrument measures distance to a reflecting object by emitting timed pulses of light and measuring the time difference between the emission of a laser pulse and the reception of the pulse's reflection(s). The measured time interval for each reflection is converted to distance, which when combined with position and altitude information from a global positioning system (GPS), inertial measurement unit, and the instrument itself, allows the derivation of the 3D-point location of the reflecting target's location (Heidemann, 2014).

Basin-characteristic measurements related to stream length, stream slope, stream density, and stream order have been identified as significant variables for the estimation of flood discharges (Eash and others, 2013; Eash, 2001), flow-duration discharges (Linhart and others, 2012), and low-flow discharges (Eash and Barnes, 2012; Eash and others, 2016) in Iowa. The constant of channel maintenance (CCM) basin characteristic was a significant variable in the development of flood-estimation equations for the Des Moines Lobe landform region (flood region 1; Eash and others, 2013). CCM is a measure of drainage density calculated as a ratio of drainage area divided by the total length of all mapped streams in the basin. However, the placement of channel initiation points (the point where water begins to flow) based on lidar DEMs has always been a matter of individual interpretation, leading to variations in stream definitions between analysts (James and Hunt, 2010; Kaiser and others, 2010; Colson and others, 2006). Thus, the testing of different quantitative stream initiation methods on hydrologically enforced lidar DEMs will provide different drainage-network delineations from which basin-characteristic measurements can be evaluated for the optimization of stream-channel delineations from lidar elevation data.

[1]U.S. Geological Survey.
[2]Iowa State University.

Side-by-side testing of basin-characteristic values measured for the total drainage area versus the “effective” drainage area of basins is needed to determine which watershed delineation provides the best predictive accuracy for flood estimation. The effective drainage area represents a subset of the total watershed area and is the area that contributes streamflow under “reasonable” flow conditions for a given storm event, such as a 20- or 2-percent annual exceedance probability (AEP) 12-hour rainfall. Because the predictive accuracy of flood-estimation equations for watersheds within the Des Moines Lobe landform region (Eash and others, 2013; Eash, 2001) is the poorest in the State, research is needed to improve the accuracy of stream-channel and watershed delineations and flood estimation within the region. In response to the need to determine optimum stream-channel delineations from lidar elevation data and to update and improve the predictive accuracy of estimates of annual exceedance-probability discharges (AEPDs) for ungaged stream sites in the Des Moines Lobe landform region, the U.S. Geological Survey (USGS), in cooperation with the Iowa Department of Transportation, the Iowa Highway Research Board, and the Iowa State University, began a study in 2015.

Purpose and Scope

This report describes stream-channel and watershed delineations and basin-characteristic measurements using lidar elevation data and presents five different methods to define stream initiation points using 3-m lidar data for 17 streamgages with drainage areas less than 50 square miles (mi^2) within the Des Moines Lobe landform region in north-central Iowa. For research and testing purposes, such relatively small basins were selected for the analysis in order to include data from a larger set of streamgages in the development of the regression equations, which should provide better predictive accuracy than those equations developed with data from fewer streamgages. The five stream initiation methods evaluated include two qualitative methods and three quantitative methods in which streams were derived from profile curvature at three different initiation thresholds and one standard continuity threshold.

The stream initiation methods were then used to define channelized flow paths on the hydrologically enforced lidar DEMs, creating multiple sets of selected basin-characteristic values measured for each streamgage. The five different methods to define stream initiation were tested side-by-side for three watershed delineations: (1) the total drainage-area delineation, (2) an effective drainage-area delineation of basins based on a 2-percent AEP 12-hour rainfall, and (3) an effective drainage-area delineation based on a 20-percent AEP 12-hour rainfall. Therefore, 15 different datasets of basin-characteristic values were measured for each streamgage watershed, with the exception of streamgage 05480993. For streamgage 05480993, no streams are available for the profile curvature stream initiation methods of 1.0 and 1.75, thus complete sets of basin characteristics could be measured only for 16 streamgages for these 2 stream initiation methods.

This report presents the results of comparisons of selected basin characteristics derived from lidar data with those previously measured using Iowa StreamStats data (Eash and others, 2013; 2016). StreamStats is a USGS web-based geographic information system (GIS) application that allows a user to delineate drainage areas and calculate select basin characteristics (Ries and others, 2008). Selected measured basin-characteristic values from lidar and StreamStats were compared for the total-drainage-area watershed delineations for the 17 streamgages to aid in the determination of similar stream-channel delineations from lidar data compared to StreamStats data.

This report also presents the results of flood-estimation regression analyses to test optimum stream-channel and watershed delineations. For the 17 streamgages, AEPD estimates were updated through September 30, 2015. Regression analyses were used to identify which of the 15 sets of lidar-measured basin-characteristic values are the most significant for the estimation of 50-, 20-, 10-, 4-, 2-, 1-, 0.5-, and 0.2-percent AEPDs for the Des Moines Lobe landform region for drainage areas less than 50 mi^2. Annual exceedance probabilities formerly were reported as flood recurrence intervals expressed in years (Holmes and Dinicola, 2010).

Description of Study Area

The Des Moines Lobe landform region (fig. 1) is characteristic of a young, postglacial landscape that is unique with respect to the rest of the State (Prior, 1991). The region generally comprises low-relief terrain, accentuated by natural lakes, potholes, and marshes, where surface-water drainage typically is poorly defined and sluggish. Soils of this region generally consist of friable, calcareous loam glacial till with thick deposits of compact, uniform pebbly loam (Oschwald and others, 1965; Prior, 1991). The following description of the Des Moines Lobe landform region is from a web site of the Iowa Department of Natural Resources (IDNR) at http://www.iowadnr.gov/Conservation/Iowas-Wildlife/Iowa-Wildlife-Action-Plan:

> “The Des Moines Lobe (Prairie Potholes) has a landscape that is gently rolling, with abundant moraines, shallow wetland basins or potholes, and a few relatively deep natural lakes. This landform retains the imprints of recent glacial occupation. Loess is entirely absent. The most prominent landform patterns left by the Wisconsin glacier on the Des Moines Lobe are the end moraines. The Des Moines Lobe is part of the Prairie Pothole Region that extends north and west into western Minnesota, eastern North and South Dakota, and the Canadian Prairie Provinces. Most of the potholes have been drained with ditching and underground tile lines to make way for agriculture. Agriculture was also responsible for greatly increasing the rate at which streams and drainage patterns developed in this geologically young landform.”

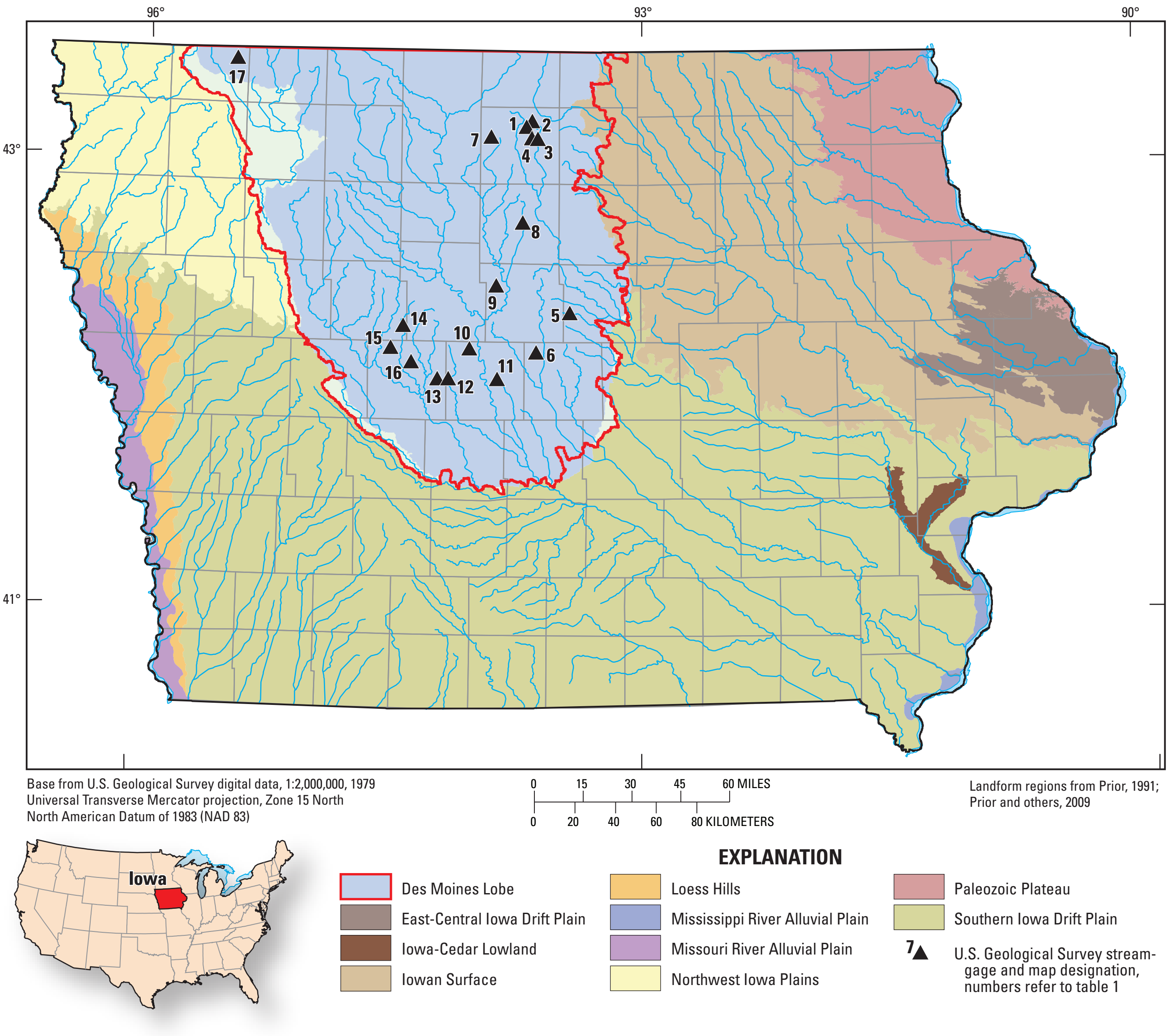

Figure 1. Des Moines Lobe landform region and U.S. Geological Survey streamgages included in this study.

Hydrologic Conditioning of Lidar DEMs

The definitions of “hydrologic processing,” (or conditioning, flattening, and enforcing) as defined in Heidemann (2014) will be used throughout this report. The DEMs used in this study were hydrologically conditioned using the method of Gelder (2015) to reflect connectivity as it exists on the land surface. Hydrologic flattening was not undertaken as part of this process, which leaves DEMs that still have triangulation artifacts in areas of voids; however, that will not affect the flow networks derived in the low-order streams of this study.

In general terms, the process of conditioning can be described as follows. First, 3-m horizontal resolution DEMs are generated by removing all one-cell sinks and a limited amount of smoothing by use of an ArcGIS terrain (Esri, 2014); these DEMs are hereafter referred to as “pit-filled.” The pit-filled DEMs are then subjected to an iterative process of “hole-punching,” whereby all depressions shallower than 9-centimeters (one-half the root mean square error and smaller than 100 square meters) are removed by using a filling process. The hole-punching process defines a number of fill-regions in which fill greater than the threshold is necessary to create flow. These fill-regions are then evaluated for the ease with which they can be made to flow. The fill-regions can be analyzed for the distances from the deepest points in the fill-region to the local watershed boundary, and these distances can serve as criteria for propensity to flow. The assumption is made that anthropogenic impediments to flow, such as roads, bridges, ditches, and terraces are roughly symmetrical in design, and if a similar or lower elevation connection can be made within a multiple (three times) of the distance from the deepest points to a valid drainage pathway, then an enforcement is made. This search radius is increased by the width of the feature to be crossed in areas of severely modified drainage, such as divided highways and railyards. The enforcement is assigned along the path of minimum cut and (or) fill between upstream and downstream cells.

Total drainage area was defined to be all cells that drain to a streamgage in a conditioned and filled DEM. This processing raises the level of all depressions and lakes within the watershed to the minimum elevation at which they would flow.

Effective drainage areas were calculated from the conditioned DEMs and AEP rainfall depths for 12-hour storm durations. Twelve-hour storm durations were chosen because this duration best approximates the average time of concentration for these watersheds (Eash, 2015). Time of concentration is the time required for runoff to travel from the most distant point in the watershed to its outlet. Annual exceedance probabilities of 2 and 20 percent were used in this analysis, resulting in rainfall depths ranging from 3.20 to 3.44 inches for the 20 percent AEP and from 5.68 to 6.23 inches for the 2 percent AEP (Perica and others, 2013). The rainfall was assumed to fall on saturated soils, resulting in instantaneous runoff. Each fill-region in the watershed was evaluated for its ability to store the volume of water resulting from the given storm’s rainfall depth. If a fill-region was not able to store all the water, it was considered filled, and flow proceeded downstream to the next fill-region; however, water volume stored in any upstream fill-regions was retained. This analysis proceeded iteratively downstream until there were no additional fill-regions to overflow. This process was conducted individually for each watershed and AEP combination, resulting in effective drainage areas for each AEP. A visual comparison of the three different drainage areas can be seen in figure 2.

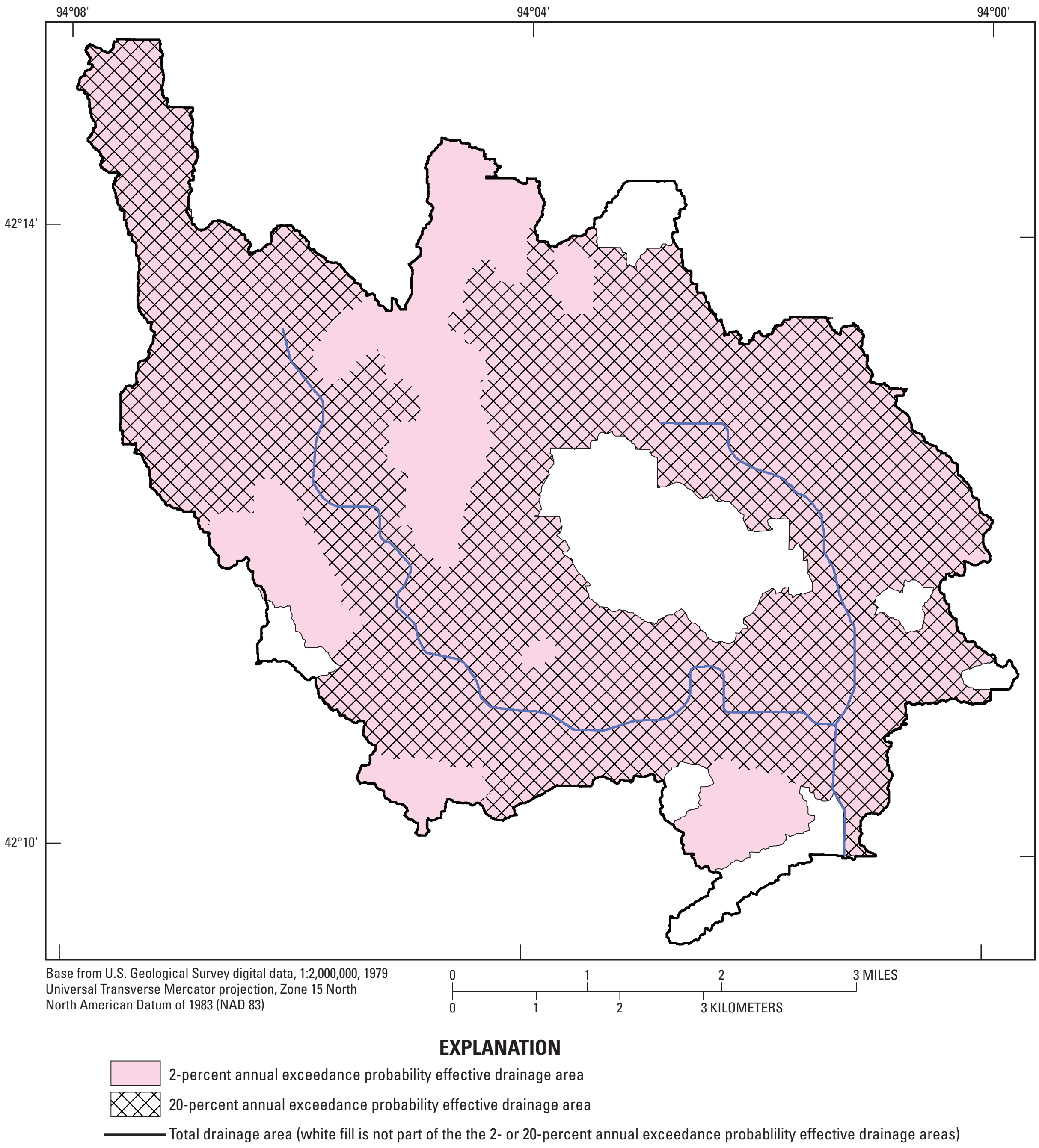

Figure 2. Example of total drainage area (23.27 square miles), 2-percent annual exceedance probability effective drainage area (20.40 square miles), and 20-percent annual exceedance probability effective drainage area (16.64 square miles) for hydrologic unit code 12 071000040703 (05481510, Bluff Creek at Pilot Mound, Iowa, site 10 in figure 1).

Stream Initiation Methods

Five different stream initiation methods were investigated. Two were qualitative (fig. 3*A*) methods based on: (1) streams derived from National Hydrography Datasets (NHD) data (https://nhd.usgs.gov) and (2) streams derived by the IDNR as part of the Federal Emergency Management Agency Digital Flood Insurance Rate Map update process conducted by Iowa Institute of Hydraulic Research (IIHR)-Hydroscience and Engineering at the University of Iowa, College of Engineering (http://www.iihr.uiowa.edu/research/iowa-flood-center/the-iowa-floodplain-mapping-project/ and http://www.iowadnr.gov/Environmental-Protection/Land-Quality/Flood-Plain-Management/Flood-Plain-Mapping). The other three stream initiation methods were quantitative and were based on thresholds of profile curvature initiation and requirements for curvature continuity (fig. 3*B*). The three quantitative methods were based on: (3) streams derived from a minimum profile curvature threshold of 0.5, (4) streams derived from a minimum profile curvature threshold of 1.0, and (5) streams derived from a minimum profile curvature threshold of 1.75 (fig. 3*B*).

Streams Derived from the National Hydrography Dataset

One set of stream initiation points was derived from the NHD. The NHD is a national framework for assigning stream-reach addresses to water-related entities, such as industrial discharges, drinking-water supplies, fish habitat areas, and wild and scenic rivers. Reach addresses establish the locations of these entities relative to one another within the NHD surface-water drainage network, much like addresses on streets. Once linked to the NHD by their reach addresses, the upstream-downstream relations of these water-related entities—and any associated information about them—can be analyzed using software tools ranging from spreadsheets to GIS. The NHD data product used in this study is the “blue lines” (the topographic expressions of stream channels) from the high-resolution NHD, generally developed at 1:24,000 or 1:12,000 scale. The blue lines indicate areas where flowing water is present most of the year except during drought.

The upstream point of each stream within the watershed was extracted, and a 50-m search radius around each initiation point was then used to find the area of maximum flow accumulation from the conditioned lidar DEM. From the initiation point, the stream was traced downstream to the streamgage. The flow path then was converted to a stream feature using Esri’s “Stream To Feature” tool with the default parameters (Esri, 2014).

Streams from the Iowa Department of Natural Resources

The streams derived from IDNR data were derived from the Iowa lidar collection and 1-m color infrared imagery collected in the spring of 2009. The GIS linework was created by the IDNR to support the Federal Emergency Management Agency Digital Flood Insurance Rate Map revision process conducted by IIHR-Hydroscience and Engineering at the University of Iowa, College of Engineering. The GIS linework was attributed so that a local resolution version of the NHD could be created later. Data at local resolution are generally considered accurate at the scale of 1:5,000.

Similar to the NHD stream initiation procedure, the upstream end of each stream within the watershed was extracted, and a 50-m search radius around each initiation point was used to find the area of maximum flow accumulation from the conditioned lidar DEM. From the initiation point, the stream was traced downstream to the streamgage. The flow path then was converted to a stream feature using Esri’s “Stream To Feature” tool with the default parameters (Esri, 2014).

Streams Derived from Profile Curvature

The profile curvature used was Esri ArcMap profile curvature, which is calculated using a 3-by-3 cell window (Esri, 2014). Normally, surface curvature is a measurement of curvature in all directions. Profile curvature is the curvature parallel to the direction of maximum slope (planform curvature is the other, perpendicular component). Profile curvature is thus a good metric for finding areas that, when positive, have a shape similar to that of water-conveying channels. Negative profile curvature is commonly found in areas like levees or terraces. Streams derived from profile curvature were determined by multiple thresholds. These thresholds include the minimum profile curvature threshold, a minimum stream length, and a maximum distance that can be crossed where curvature is below the threshold. The minimum profile curvature thresholds used in this study were 0.5, 1.0, and 1.75. The minimum stream length threshold was set at 100 m and was estimated by reviewing the minimum stream lengths within the NHD and IDNR stream databases in the area of interest. The maximum distance that could be crossed, where curvature was below the threshold was also set at 100 m, and connectivity was evaluated from each streamgage location.

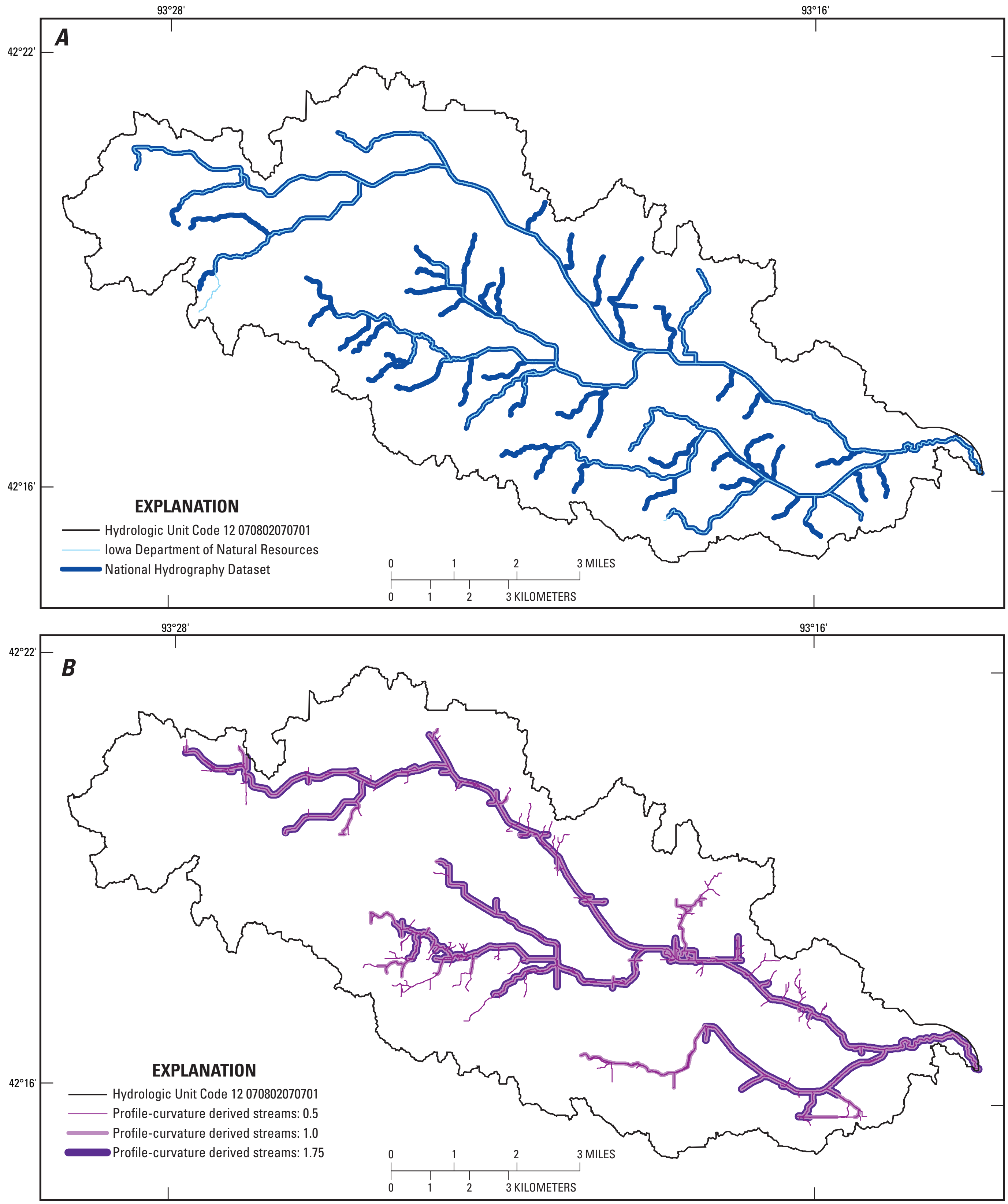

Figure 3. Examples of derived streams for hydrologic unit code 12 070802070701 (0545129280, Honey Creek Tributary near Radcliffe, Iowa, site 5 in figure 1) from initiation methods based on *A*, the National Hydrography Dataset and the Iowa Department of Natural Resources and *B*, three thresholds of profile curvature and requirements for continuity.

Dataset Development for Streamgages

Data used in this report were collected for 16 crest-stage gages and 1 continuous-record streamgage with drainage areas less than 50 mi^2 that are within the Des Moines Lobe landform region (fig. 1, table 1). All 17 streamgages were also included in the 2013 StreamStats flood-estimation study for Iowa, in which 59 selected basin characteristics were measured for each streamgage by using 1:24,000-scale topographic-map data from stream networks, basin boundaries, and 10-m DEMs (Eash and others, 2013).

Processing of Lidar DEMs and Measurement of Basin Characteristics

Basin characteristics investigated in this study as potential explanatory variables in the regression analysis were selected based on the results from previous studies in similar hydrologic areas and the ability to quantify the basin characteristics using GIS technology and digital datasets. Hydrologic characteristics initially were computed as observed values for 208 continuous-record streamgages by using daily mean discharge data. The hydrologic characteristics subsequently were mapped by using a kriging procedure to compute interpolated values for a low-flow simulation study performed for Iowa (Eash and Barnes, 2012). A list of the 208 streamgages included in the low-flow study, descriptions of the hydrologic-characteristic computations and the kriging procedure, and isoline maps created from kriged grids for three of the five hydrologic characteristics are presented in Eash and Barnes (2012). The pedologic, geologic, and land-use characteristics were computed from the National Resources Conservation Service Soil Survey Geographic database (SSURGO) (Soil Survey Staff, 2012) for seven soil characteristics, from the Iowa Geological Survey-IDNR Des Moines Lobe landform region boundary for the Des Moines Lobe geologic characteristic (Prior and others, 2009), and from the Multi-Resolution Land Characteristics Consortium 2011 National Land Cover Database (Multi-Resolution Land Characteristics Consortium, 2011) for the land-use characteristics that measured the percentage of area of row crops (http://www.mrlc.gov/index.php; Homer and others, 2004). The climatic characteristics were computed from Oregon State University Parameter-elevation Regressions on Independent Slopes Model (PRISM) datasets (PRISM Climate Group, 2008) and from the National Oceanic and Atmospheric Administration (NOAA) Precipitation-Frequency Atlas of the United States, Midwestern States (Perica and others, 2013).

Additional data layers were generated to calculate basin characteristics to develop the regional regression equations (RREs) for estimating AEPDs for Iowa. These primary base-grid data layers include catchments, flow accumulation, flow direction, and an artificial flow-path grid used to delineate drainage basins. These additional layers then were used to create layers that control the delineation of a watershed, subwatersheds, and stream networks within these drainage basins, including the created layers named AdjointCatchment, which is a polygon representing the whole upstream area draining to its inlet point for each catchment that is not a head catchment; Catchment, which is an elementary drainage area produced by subdivision of the landscape using a consistent set of physical rules; DrainageLine, which is the line through the centers of the DEM cells on a drainage path; DrainagePoint, which is the point at the center of a DEM cell at the most downstream location within a drainage area; LongestFlowPathCat, which is the longest flow path for each catchment; and LongestFlowPathAdjCat, which is the longest flow path for each adjoint catchment (Esri, 2014).

In addition, all of the streams from each of the initiation methods were run through two additional processing steps to remove any bias from the stair-stepping effect from earlier processing steps that would cause an increase in stream length. First, streams were smoothed with a tolerance of 30 m using Esri's "Smooth Line" tool with the default parameters, and then streams were generalized to remove the exaggerated stair-stepping effect (Esri, 2014). In addition, the DEM was resampled to 150 m for use in the basin-length measurement to assist with speed of the calculation.

All 58 basin characteristics listed in table 2 were measured using ArcHydro for ArcGIS 10.2 (version 10.2, March 30, 2015) or Spatial Analyst tools in ArcGIS, version 10.3.1 for Desktop (Esri, 2014).

Annual Exceedance-Probability Discharges

The AEPDs were estimated for each of the 17 streamgages from observed streamflow data using a probability-analysis method named the expected moments algorithm/multiple Grubbs-Beck test, hereafter referred to as the EMA/MGB analysis method (Cohn and others, 1997, 2001, 2013; Eash and others, 2013). Annual peak-discharge records collected through the 2015 water year were retrieved for the 17 streamgages from the USGS National Water Information System database (U.S. Geological Survey, 2016). A water year is the 12-month period October 1 through September 30 and is designated by the year in which it ends. The number of annual peak discharges, or systematic peaks, collected at the 17 streamgages with drainage areas less than 50 mi^2 that were used in the EMA/MGB analyses ranged from 13 to 60 years, with an average of 35 years and a median of 37 years (table 1). The Interagency Advisory Committee on Water Data (1982) recommends a minimum of 10 years to estimate AEPDs.

The AEPDs for streamgages are calculated from an AEP analysis that relates observed annual peak discharges to the AEPs. Estimates of AEPDs at streamgages change as additional annual peak discharges are measured; EMA/MGB estimates of AEPDs can be updated and become more statistically reliable. The EMA/MGB analysis method within the USGS PeakFQ, (version 7.1) program (Cohn and others, 1997, 2001, 2013; Eash and others, 2013; Veilleux and others, 2014) and the results of a recent statewide regional skew study (Veilleux and others, 2012; Eash and others, 2013) were used to estimate AEPDs at the 17 streamgages. EMA/MGB estimates calculated through the 2015 water year at the 17 streamgages for AEPs of 50, 20, 10, 4, 2, 1, 0.5, and 0.2 percent are listed in table 1.

Table 1. Streamgage information included in this study.

[no., number; mi², square miles; EMA/MGB, expected moments algorithm/multiple Grubbs-Beck test (Cohn and others, 1997, 2001, 2013; Eash and others, 2013); DRNAREA, drainage area; CSG, crest stage gage; CON, continuous stream gage]

Map no. (fig. 1)	Streamgage number	Streamgage name	Type of streamgage	Published drainage area (Lara, 1987) (mi²)	Systematic peaks in EMA/MGB analysis (years)	Historical period of EMA/MGB analysis	Historical period length of EMA/MGB analysis (years)	Estimates of annual exceedance-probability discharges, in cubic feet per second								Basin characteristic from StreamStats used to develop best lidar regression equations in table 6
								50 percent	20 percent	10 percent	4 percent	2 percent	1 percent	0.5 percent	0.2 percent	DRNAREA (mi²)
1	05448600	East Branch Iowa River above Hayfield	CSG	2.23	60	1953–2015	63	31.2	119	220	402	577	781	1,020	1,370	1.12
2	05448700	East Branch Iowa River near Hayfield	CSG	7.94	37	1952–91	40	111	222	309	426	518	612	707	835	5.69
3	05448800	East Branch Iowa River at Garner	CSG	45.1	40	1952–91	40	312	629	873	1,200	1,460	1,720	1,980	2,330	37.89
4	05448900	East Branch Iowa River Tributary near Garner	CSG	5.98	34	1952–86	35	43.3	134	227	381	519	675	848	1,100	2.55
5	0545129280	Honey Creek Tributary near Radcliffe	CSG	3.29	24	1991–2015	25	172	388	569	831	1,040	1,270	1,500	1,820	2.32
6	05469990	Keigley Branch near Story City	CSG	31.0	50	1966–2015	50	424	1,150	1,830	2,920	3,880	4,940	6,100	7,780	26.15
7	0548065350	Drainage Ditch 97 Tributary near Britt	CSG	0.94	21	1991–2015	25	41.9	131	225	386	536	710	908	1,210	0.85
8	05480930	White Fox Creek at Clarion	CSG	13.3	49	1966–2015	49	253	733	1,200	1,940	2,590	3,300	4,070	5,160	9.07
9	05480993	Brewers Creek Tributary near Webster City	CSG	1.58	26	1990–2015	26	108	260	391	582	737	900	1,070	1,300	1.66
10	05481510	Bluff Creek at Pilot Mound	CSG	23.5	50	1966–2015	50	324	705	1,010	1,450	1,790	2,150	2,510	3,000	16.64
11	05481528	Peas Creek Tributary at Boone	CSG	0.30	13	1990–2003	14	48.2	110	165	249	322	402	491	621	0.27
12	05481680	Beaver Creek at Beaver	CSG	38.5	25	1966–90	25	669	1,060	1,330	1,680	1,940	2,200	2,470	2,820	32.71
13	05481690	West Beaver Creek at Grand Junction	CSG	12.6	24	1966–89	24	117	376	660	1,160	1,640	2,210	2,870	3,900	13.84
14	05482600	Hardin Creek at Farnhamville	CSG	43.7	39	1952–90	39	481	992	1,400	1,980	2,450	2,930	3,440	4,140	36.35
15	05482800	Happy Run at Churdan	CSG	7.58	39	1951–89	39	32.5	85.6	134	209	271	339	411	512	6.39
16	05483000	East Fork Hardin Creek near Churdan	CON	24.0	40	1952–91	40	228	369	463	580	665	747	827	930	16.88
17	06604584	Dry Run Creek near Harris	CSG	4.30	22	1990–2015	26	228	376	477	604	696	787	876	992	4.04

Table 2. Basin characteristics tested for significance in developing regression equations.

[DEM, digital elevation model; m, meter; WBD, Watershed Boundary Dataset (https://nhd.usgs.gov/wbd.html); 24K, 1:24,000-scale; π, pi a mathematical constant commonly approximated as 3.14; NHD, National Hydrography Dataset (https://nhd.usgs.gov)]

Morphometric characteristics	Source data
DRNAREA–Drainage area (square miles)	DEM (10 m) http://nationalmap.gov/elevation.html; WBD (24K) https://gdg.sc.egov.usda.gov/
BASINPERIM–Basin perimeter (miles)	DEM (10 m) http://nationalmap.gov/elevation.html; WBD (24K) https://gdg.sc.egov.usda.gov/
LFPLENGTH–Length of longest flow path as measured from basin outlet to basin divide (miles)	DEM (10 m) http://nationalmap.gov/elevation.html; NHD (24K) http://nhd.usgs.gov/
BASLENAH–Basin length (miles), measured along a line areally centered through the basin polygon from end points of LFPLENGTH	DEM (150 m) http://nationalmap.gov/elevation.html; WBD (24K) https://gdg.sc.egov.usda.gov/
BSLDEM10M–Average basin slope computed from 10-meter DEM (percent)	DEM (10 m) http://nationalmap.gov/elevation.html
RELIEF–Basin relief computed as maximum elevation minus minimum elevation (feet)	DEM (10 m) http://nationalmap.gov/elevation.html
RELRELF–Relative relief computed as RELIEF divided by BASINPERIM (feet per mile)	DEM (10 m) http://nationalmap.gov/elevation.html; WBD (24K) https://gdg.sc.egov.usda.gov/
BSHAPE–Shape factor measure of basin shape computed as BASLENAH squared divided by DRNAREA (dimensionless)	DEM (10 m) http://nationalmap.gov/elevation.html; WBD (24K) https://gdg.sc.egov.usda.gov/
ELONGRATIO–Elongation ratio measure of basin shape, ratio of (1) the diameter of a circle of area equal to that of the basin to (2) the length of the basin, ELONGRATIO = [4 DRNAREA/π (BASLENAH)2]0.5 (dimensionless)	DEM (10 m) http://nationalmap.gov/elevation.html; WBD (24K) https://gdg.sc.egov.usda.gov/
ROTUND–Rotundity of basin measure of basin shape, ROTUND = [π (BASLENAH)2]/[4 (DRNAREA)] (dimensionless)	DEM (10 m) http://nationalmap.gov/elevation.html; WBD (24K) https://gdg.sc.egov.usda.gov/
COMPRAT–Compactness ratio measure of basin shape, is the ratio of the perimeter of the basin to the circumference of a circle of equal area, COMPRAT = BASINPERIM/2 (π DRNAREA)0.5 (dimensionless)	DEM (10 m) http://nationalmap.gov/elevation.html; WBD (24K) https://gdg.sc.egov.usda.gov/
MCSRBSFT–Main-channel sinuosity ratio computed as LFPLENGTH divided by BASLENAH (dimensionless)	DEM (10 m) http://nationalmap.gov/elevation.html; WBD (24K) https://gdg.sc.egov.usda.gov/; NHD (24K) http://nhd.usgs.gov/
STRMTOT–Total length of mapped streams in basin (miles)	DEM (10 m) http://nationalmap.gov/elevation.html; NHD (24K) http://nhd.usgs.gov/
STRDEN–Stream density computed as STRMTOT divided by DRNAREA (miles per square mile)	DEM (10 m) http://nationalmap.gov/elevation.html; WBD (24K) https://gdg.sc.egov.usda.gov/; NHD (24K) http://nhd.usgs.gov/
SLENRAT–Slenderness ratio computed as LFPLENGTH squared divided by DRNAREA (dimensionless)	DEM (10 m) http://nationalmap.gov/elevation.html; WBD (24K) https://gdg.sc.egov.usda.gov/; NHD (24K) http://nhd.usgs.gov/
CCM–Constant of channel maintenance computed as DRNAREA divided by STRMTOT (square miles per mile)	DEM (10 m) http://nationalmap.gov/elevation.html; WBD (24K) https://gdg.sc.egov.usda.gov/; NHD (24K) http://nhd.usgs.gov/
CSL1085LFP–Stream slope computed as the change in elevation between points 10 and 85 percent of length of LFPLENGTH divided by length between the points (feet per mile)	DEM (10 m) http://nationalmap.gov/elevation.html; NHD (24K) http://nhd.usgs.gov/
CSL100–Stream slope computed as entire LFPLENGTH (feet per mile)	DEM (10 m) http://nationalmap.gov/elevation.html; NHD (24K) http://nhd.usgs.gov/
MCSP–Main-channel slope proportion computed as LFPLENGTH divided by the square root of CSL1085LFP (dimensionless)	DEM (10 m) http://nationalmap.gov/elevation.html; NHD (24K) http://nhd.usgs.gov/
RUGGED–Ruggedness number computed as STRDEN multiplied by RELIEF (feet per mile)	DEM (10 m) http://nationalmap.gov/elevation.html; WBD (24K) https://gdg.sc.egov.usda.gov/; NHD (24K) http://nhd.usgs.gov/
SLOPERAT–Slope ratio computed as CSL1085LFP divided by BSLDEM10M (dimensionless)	DEM (10 m) http://nationalmap.gov/elevation.html; NHD (24K) http://nhd.usgs.gov/
FOSTREAM–Number of first-order streams within basin using the Strahler stream ordering method (dimensionless)	DEM (10 m) http://nationalmap.gov/elevation.html; NHD (24K) http://nhd.usgs.gov/
DRNFREQ–Drainage frequency computed as FOSTREAM divided by DRNAREA (number of first-order streams per square mile)	DEM (10 m) http://nationalmap.gov/elevation.html; WBD (24K) https://gdg.sc.egov.usda.gov/; NHD (24K) http://nhd.usgs.gov/
RSD–Relative stream density computed as FOSTREAM multiplied by DRNAREA and divided by STRMTOT squared (dimensionless)	DEM (10 m) http://nationalmap.gov/elevation.html; WBD (24K) https://gdg.sc.egov.usda.gov/; NHD (24K) http://nhd.usgs.gov/
SLOP30_10M–Percent area with slopes greater than 30 percent from 10-meter DEM	DEM (10 m) http://nationalmap.gov/elevation.html
NFSL30_10M–Percent area with north-facing slopes greater than 30 percent from 10-meter DEM	DEM (10 m) http://nationalmap.gov/elevation.html
PFLATTOT–Total percent flat land (slope less than 1 percent) in watershed (percent)	http://water.usgs.gov/GIS/metadata/usgswrd/XML/hlrus.xml
PFLATLOW–Percent flat land (slope less than 1 percent) in watershed lowland (elevation less than midpoint between minimum and maximum elevation) (percent)	http://water.usgs.gov/GIS/metadata/usgswrd/XML/hlrus.xml
PFLATUP–Percent flat land (slope less than 1 percent) in watershed upland (elevation greater than or equal to midpoint between minimum and maximum elevation) (percent)	http://water.usgs.gov/GIS/metadata/usgswrd/XML/hlrus.xml

Table 2. Basin characteristics tested for significance in developing regression equations.—Continued

[DEM, digital elevation model; m, meter; WBD, Watershed Boundary Dataset (https://nhd.usgs.gov/wbd.html); 24K, 1:24,000-scale; π, pi a mathematical constant commonly approximated as 3.14; NHD, National Hydrography Dataset (https://nhd.usgs.gov)]

Morphometric characteristics	Source data
Pedologic/geologic/land-use characteristics	
SSURGOA–Percent area underlain by hydrologic soil type A (percent area)	http://websoilsurvey.sc.egov.usda.gov/
SSURGOB–Percent area underlain by hydrologic soil type B (percent area)	http://websoilsurvey.sc.egov.usda.gov/
SSURGOC–Percent area underlain by hydrologic soil type C (percent area)	http://websoilsurvey.sc.egov.usda.gov/
SSURGOD–Percent area underlain by hydrologic soil type D (percent area)	http://websoilsurvey.sc.egov.usda.gov/
SSURGOSAND–Percent volume of sand content of soil (percent volume)	http://websoilsurvey.sc.egov.usda.gov/
SSURGOCLAY–Percent volume of clay content of soil (percent volume)	http://websoilsurvey.sc.egov.usda.gov/
SSURGOKSAT–Average soil permeability or saturated hydraulic conductivity of soil (micrometers per second)	http://websoilsurvey.sc.egov.usda.gov/
DESMOIN–Percent area of basin within Des Moines Lobe landform region (percent area)	https://programs.iowadnr.gov/nrgislibx/
LC11ACROP–Percent area of cultivated crops from NLCD 2011 class 82 (percent area)	http://www.mrlc.gov/nlcd2011.php
LC11ADECID–Percent area of deciduous forest from NLCD 2011 class 41 (percent area)	http://www.mrlc.gov/nlcd2011.php
LC11APAST–Percent area of pasture/hay from NLCD 2011 class 81 (percent area)	http://www.mrlc.gov/nlcd2011.php
LC11CRPHAY–Percent area of cultivated crops and hay from NLCD 2011 classes 81 and 82 (percent area)	http://www.mrlc.gov/nlcd2011.php
LC11AWETL–Percent area of wetlands from NLCD 2011 classes 90 and 95 (percent area)	http://www.mrlc.gov/nlcd2011.php
LC11IMP–Percent area of impervious area from NLCD 2011 impervious data set (percent area)	http://www.mrlc.gov/nlcd2011.php
LC11DEV–Percent area of developed area from NLCD 2011 classes 21–24 (percent area)	http://www.mrlc.gov/nlcd2011.php
Climatic characteristics	
PRECIP–Mean annual precipitation 1981–2010 (inches)	http://www.prism.oregonstate.edu/normals/
MW2Y24H–Maximum 24-hour precipitation that occurs on average once in 2 years	http://www.nws.noaa.gov/oh/hdsc/PF_documents/Atlas14_Volume8.pdf
MW5Y24H–Maximum 24-hour precipitation that occurs on average once in 5 years	http://www.nws.noaa.gov/oh/hdsc/PF_documents/Atlas14_Volume8.pdf
MW10Y24H–Maximum 24-hour precipitation that occurs on average once in 10 years	http://www.nws.noaa.gov/oh/hdsc/PF_documents/Atlas14_Volume8.pdf
MW25Y24H–Maximum 24-hour precipitation that occurs on average once in 25 years	http://www.nws.noaa.gov/oh/hdsc/PF_documents/Atlas14_Volume8.pdf
MW50Y24H–Maximum 24-hour precipitation that occurs on average once in 50 years	http://www.nws.noaa.gov/oh/hdsc/PF_documents/Atlas14_Volume8.pdf
MW100Y24H–Maximum 24-hour precipitation that occurs on average once in 100 years	http://www.nws.noaa.gov/oh/hdsc/PF_documents/Atlas14_Volume8.pdf
MW200724H–Maximum 24-hour precipitation that occurs on average once in 200 years	http://www.nws.noaa.gov/oh/hdsc/PF_documents/Atlas14_Volume8.pdf
MW500Y24H–Maximum 24-hour precipitation that occurs on average once in 500 years	http://www.nws.noaa.gov/oh/hdsc/PF_documents/Atlas14_Volume8.pdf
MAYAVEPRE–Mean May precipitation 1981–2010 (inches)	http://www.prism.oregonstate.edu/normals/
JUNEAVPRE–Mean June precipitation 1981–2010 (inches)	http://www.prism.oregonstate.edu/normals/
JULYAVPRE–Mean July precipitation 1981–2010 (inches)	http://www.prism.oregonstate.edu/normals/
PRMAYJUN10–Mean May through July precipitation 1981–2010 (inches)	http://www.prism.oregonstate.edu/normals/
PMPE–Mean annual precipitation minus potential evapotranspiration (millimeters)	http://water.usgs.gov/GIS/metadata/usgswrd/XML/hlrus.xml

Comparison of Lidar and StreamStats Basin Characteristics

Hydrologically enforced lidar DEMs were created for 13 selected 12-digit hydrologic unit codes (HUCs) (https://water.usgs.gov/GIS/huc.html) in the Des Moines Lobe landform region for use in this study. Completion of hydrologically enforced lidar DEMs and completion of all the processing steps to measure basin characteristics for the 401 other 12-digit HUCs in the Des Moines Lobe landform region (flood region 1) would be needed before the RREs developed in this study could be implemented in StreamStats.

Basin characteristics measured for the 17 streamgages using lidar data for 3 different stream-initiation methods, and basin characteristics measured for 16 streamgages for 2 different stream-initiation methods, were compared to those measured using StreamStats data to identify the lidar stream networks that are most similar to StreamStats stream networks. The lidar basin characteristics were measured using the ArcHydro-Tools processed lidar DEMs. The StreamStats basin characteristics were measured using 1:24,000-scale topographic-map data from NHD High Resolution stream networks (https://nhd.usgs.gov), Watershed Boundary Dataset (WBD) (https://nhd.usgs.gov/wbd.html) basin boundaries, and 10-m DEMs (Eash and others, 2013). Basin characteristics measured using lidar delineations of total drainage areas and StreamStats delineations of total GIS-determined drainage areas (DRNAREA) were compared for the 17 streamgages.

DRNAREA and six additional morphometric basin characteristics listed in table 2 were selected to represent measurements of stream-channel length, density, and order for evaluating which of the five different lidar stream-initiation methods appear to provide results most similar to those obtained from analyses of stream networks from 1:24,000-scale topographic map (StreamStats) data. The six morphometric basin characteristics include: (1) total length of all mapped streams in the basin (STRMTOT), (2) stream density (STRDEN), (3) CCM, (4) number of first-order streams (FOSTREAM) within the basin using the Strahler stream ordering method (Strahler, 1952; Horton, 1945), (5) drainage frequency (DRNFREQ), and (6) relative stream density (RSD). Basin-characteristic names used in this study were selected to maintain consistency with the names applied to explanatory variables in the USGS StreamStats web-based GIS application (https://streamstatsags.cr.usgs.gov/ss_defs/basin_char_defs.aspx).

Basin-characteristic values measured for the 2013 Iowa peak-flow study (Eash and others, 2013) were used for the StreamStats basin characteristics. Values for two of the six StreamStats basin characteristics (STRMTOT and CCM) were published in Eash and others (2013, in table 3). Values for the four other StreamStats basin characteristics (STRDEN, FOSTREAM, DRNFREQ, and RSD) were retrieved from the ArcHydro Tools files developed for the 2013 Iowa peak-flow study, and they are presented along with the two previously published values (STRMTOT and CCM) in table 3.

The Wilcoxon signed-rank test was applied to determine the statistical significance between the median of each of the six sets of basin characteristics measured for each of the five sets of lidar stream-initiation methods to the median of the StreamStats basin characteristics by using the Comprehensive R Archive Network (CRAN) package from Modern Applied Statistics with S (MASS) program (Venables and Ripley, 2002). Results of the statistical comparison tests are shown in table 3, which also includes comparisons for DRNAREA, because it is used in the calculations for STRDEN, CCM, DRNFREQ, and RSD. Lidar values for DRNAREA are the same for the each of the five sets of lidar stream-initiation methods.

The comparison tests indicate three general results (table 3). First, there is a statistically significant difference between the median of the StreamStats measurements of DRNAREA compared to the median of the lidar measurements of DRNAREA (p-value 0.008). Second, there is no statistically significant difference between StreamStats and lidar measurements of STRMTOT, STRDEN, and CCM (p-values range 0.071 to 1.00) for any of the five sets of lidar stream-initiation methods, which indicates there is not a significant difference between StreamStats and lidar measurements of stream-channel length and stream density. Third, there is no statistically significant difference between StreamStats and lidar measurements of FOSTREAM, DRNFREQ, and RSD (p-values range 0.089 to 0.182) for only the IDNR lidar stream-initiation method. For the NHD lidar stream-initiation method, there is a statistically significant difference between StreamStats and lidar measurements only for DRNFREQ (p-value 0.003). For each of the three profile curvature stream initiation methods of 0.5, 1.0, and 1.75, there is a statistically significant difference between StreamStats and lidar measurements for FOSTREAM, DRNFREQ, and RSD (p-values range <0.001 to 0.001).

Overall results of the comparison tests appear to indicate that the IDNR lidar stream-initiation method provides stream networks that are most similar to StreamStats stream networks obtained from 1:24,000-scale topographic-map data. The NHD lidar stream-initiation method appears to provide the second most similar stream networks compared to StreamStats stream networks. The three profile curvature stream initiation methods of 0.5, 1.0, and 1.75 all provide lidar stream networks that are not statistically different from StreamStats stream networks for stream-channel length and stream density. However, all three of the profile curvature stream initiation methods are statistically different from StreamStats stream networks regarding the number of FOSTREAM and the related measurements of DRNFREQ and RSD.

Table 3. Comparison of selected lidar and StreamStats basin characteristics.

[no., number; DRNAREA, drainage area; mi^2, square mile; STRMTOT, total length of mapped streams in basin; mi, mile; STRDEN, stream density computed as STRMTOT divided by DRNAREA; CCM, constant of channel maintenance computed as DRNAREA divided by STRMTOT; FOSTREAM, number of first-order streams within basin using the Strahler stream ordering method (Strahler, 1952; Horton, 1945); DRNFREQ, drainage frequency computed as FOSTREAM divided by DRNAREA; RSD, relative stream density computed as FOSTREAM multiplied by DRNAREA]

Map no. (fig. 1)	Streamgage number	StreamStats method							NHD-derived						
		DRNAREA (mi^2)	STRMTOT (mi)	STRDEN (mi/mi^2)	CCM (mi^2/mi)	FOSTREAM	DRNFREQ (FOSTREAM/ mi^2)	RSD	DRNAREA (mi^2)	STRMTOT (mi)	STRDEN (mi/mi^2)	CCM (mi^2/mi)	FOSTREAM	DRNFREQ (FOSTREAM/ mi^2)	RSD
1	05448600	1.54	1.059	0.689	1.452	1	0.650	1.371	1.24	1.076	0.871	1.148	1	0.809	1.067
2	05448700	7.34	7.247	0.988	1.012	3	0.409	0.419	7.21	7.312	1.014	0.986	3	0.416	0.405
3	05448800	47.65	33.254	0.698	1.433	9	0.189	0.388	43.78	33.550	0.766	1.305	9	0.206	0.350
4	05448900	5.63	5.100	0.907	1.103	1	0.178	0.216	5.49	4.084	0.744	1.344	1	0.182	0.329
5	0545129280	3.40	3.820	1.124	0.890	2	0.589	0.466	2.45	4.025	1.644	0.608	2	0.817	0.302
6	05469990	31.64	36.688	1.159	0.863	21	0.664	0.494	31.29	38.946	1.245	0.803	23	0.735	0.474
7	0548065350	0.92	1.617	1.759	0.568	1	1.088	0.352	0.85	1.629	1.915	0.522	1	1.176	0.321
8	05480930	11.37	12.282	1.080	0.926	8	0.703	0.603	11.37	13.348	1.174	0.852	9	0.792	0.574
9	05480993	1.71	2.211	1.296	0.772	1	0.586	0.349	1.66	0.279	0.168	5.955	1	0.602	21.335
10	05481510	22.29	14.536	0.652	1.533	2	0.090	0.211	23.27	11.165	0.480	2.085	2	0.086	0.373
11	05481528	0.27	0.586	2.191	0.456	1	3.740	0.779	0.27	0.593	2.200	0.455	1	3.709	0.766
12	05481680	40.33	27.541	0.683	1.465	4	0.099	0.213	40.27	28.236	0.701	1.426	4	0.099	0.202
13	05481690	18.22	15.779	0.866	1.155	5	0.274	0.366	14.76	15.916	1.079	0.927	5	0.339	0.291
14	05482600	42.91	26.669	0.621	1.609	11	0.256	0.664	41.99	34.394	0.819	1.221	11	0.262	0.390
15	05482800	8.88	6.579	0.741	1.349	1	0.113	0.205	8.66	6.721	0.776	1.289	4	0.462	0.767
16	05483000	23.41	6.054	0.259	3.866	2	0.085	1.277	23.31	8.356	0.359	2.789	2	0.086	0.668
17	06604584	4.84	5.594	1.155	0.865	3	0.620	0.464	4.04	5.738	1.421	0.704	3	0.743	0.368
Wilcoxon signed-rank test p-value[1]									[2] 0.0083	0.0887	0.0714	0.1202	[2] 0.1814	[2] 0.0032	0.2842
Percent of sites where the methods did not agree.									88.2	100.0	100.0	100.0	17.6	94.1	100.0

Table 3. Comparison of selected lidar and StreamStats basin characteristics.—Continued

[no., number; DRNAREA, drainage area; mi^2, square mile; STRMTOT, total length of mapped streams in basin; mi, mile; STRDEN, stream density computed as STRMTOT divided by DRNAREA; CCM, constant of channel maintenance computed as DRNAREA divided by STRMTOT; FOSTREAM, number of first-order streams within basin using the Strahler stream ordering method (Strahler, 1952; Horton, 1945); DRNFREQ, drainage frequency computed as FOSTREAM divided by DRNAREA; RSD, relative stream density computed as FOSTREAM multiplied by DRNAREA]

Map no. (fig. 1)	Streamgage number	IDNR-derived							Profile curvature 0.5 threshold method						
		DRNAREA (mi^2)	STRMTOT (mi)	STRDEN (mi/mi^2)	CCM (mi^2/mi)	FOSTREAM	DRNFREQ (FOSTREAM/ mi^2)	RSD	DRNAREA (mi^2)	STRMTOT (mi)	STRDEN (mi/mi^2)	CCM (mi^2/mi)	FOSTREAM	DRNFREQ (FOSTREAM/ mi^2)	RSD
1	05448600	1.24	1.126	0.911	1.097	1	0.809	0.975	1.24	1.888	1.528	0.654	7	5.666	2.427
2	05448700	7.21	7.418	1.029	0.972	3	0.416	0.393	7.21	11.641	1.614	0.619	37	5.131	1.969
3	05448800	43.78	34.212	0.781	1.280	11	0.251	0.411	43.78	49.827	1.138	0.879	127	2.901	2.240
4	05448900	5.49	4.084	0.744	1.344	1	0.182	0.329	5.49	3.449	0.629	1.591	8	1.458	3.690
5	0545129280	2.45	2.836	1.158	0.863	1	0.408	0.304	2.45	0.654	0.267	3.745	3	1.225	17.185
6	05469990	31.29	24.285	0.776	1.289	17	0.543	0.902	31.29	36.140	1.155	0.866	125	3.995	2.995
7	0548065350	0.85	1.137	1.337	0.748	1	1.176	0.657	0.85	1.514	1.780	0.562	5	5.880	1.855
8	05480930	11.37	12.530	1.102	0.907	8	0.704	0.579	11.37	13.469	1.185	0.844	40	3.518	2.507
9	05480993	1.66	0.424	0.255	3.920	1	0.602	9.247	1.66	1.068	0.642	1.557	2	1.203	2.916
10	05481510	23.27	11.165	0.480	2.085	6	0.258	1.120	23.27	21.832	0.938	1.066	59	2.535	2.881
11	05481528	0.27	0.603	2.235	0.447	2	7.417	1.485	0.27	1.967	7.295	0.137	7	25.961	0.488
12	05481680	40.27	38.491	0.956	1.046	11	0.273	0.299	40.27	63.324	1.572	0.636	187	4.644	1.878
13	05481690	14.76	17.879	1.212	0.825	10	0.678	0.462	14.76	32.543	2.205	0.453	88	5.964	1.226
14	05482600	41.99	34.892	0.831	1.204	16	0.381	0.552	41.99	59.846	1.425	0.702	171	4.072	2.005
15	05482800	8.66	2.050	0.237	4.225	1	0.115	2.060	8.66	2.088	0.241	4.150	2	0.231	3.975
16	05483000	23.31	5.100	0.219	4.570	1	0.043	0.896	23.31	8.607	0.369	2.708	23	0.987	7.237
17	06604584	4.04	3.055	0.757	1.322	2	0.495	0.865	4.04	3.853	0.954	1.048	8	1.981	2.176
		[2] 0.0083	0.4307	0.4586	0.2842	[2] 0.1817	[2] 0.0928	0.0887	[2] 0.0083	0.1324	0.1594	0.3778	[2] 0.0003	0.0000	0.0000
		88.2	100.0	100.0	100.0	58.8	100.0	100.0	88.2	100.0	100.0	100.0	100.0	100.0	100.0

Table 3. Comparison of selected lidar and StreamStats basin characteristics.—Continued

[no., number; DRNAREA, drainage area; mi², square mile; STRMTOT, total length of mapped streams in basin; mi, mile; STRDEN, stream density computed as STRMTOT divided by DRNAREA; CCM, constant of channel maintenance computed as DRNAREA divided by STRMTOT; FOSTREAM, number of first-order streams within basin using the Strahler stream ordering method (Strahler, 1952; Horton, 1945); DRNFREQ, drainage frequency computed as FOSTREAM divided by DRNAREA; RSD, relative stream density computed as FOSTREAM multiplied by DRNAREA]

Map no. (fig. 1)	Streamgage number	Profile curvature 1.0 threshold method							Profile curvature 1.75 threshold method						
		DRNAREA (mi²)	STRMTOT (mi)	STRDEN (mi/mi²)	CCM (mi²/mi)	FOSTREAM	DRNFREQ (FOSTREAM/mi²)	RSD	DRNAREA (mi²)	STRMTOT (mi)	STRDEN (mi/mi²)	CCM (mi²/mi)	FOSTREAM	DRNFREQ (FOSTREAM/mi²)	RSD
1	05448600	1.24	1.660	1.344	0.744	7	5.666	3.138	1.24	1.199	0.970	1.031	2	1.619	1.720
2	05448700	7.21	9.858	1.367	0.731	26	3.606	1.929	7.21	8.037	1.114	0.897	11	1.525	1.228
3	05448800	43.78	42.617	0.973	1.027	81	1.850	1.953	43.78	37.329	0.853	1.173	47	1.073	1.477
4	05448900	5.49	3.139	0.572	1.748	4	0.729	2.227	5.49	2.937	0.535	1.868	4	0.729	2.544
5	0545129280	2.45	0.514	0.210	4.762	2	0.817	18.522	2.45	0.492	0.201	4.976	1	0.408	10.113
6	05469990	31.29	21.070	0.673	1.485	58	1.853	4.088	31.29	18.037	0.576	1.735	43	1.374	4.136
7	0548065350	0.85	1.186	1.394	0.717	2	2.352	1.210	0.85	1.180	1.388	0.720	2	2.352	1.221
8	05480930	11.37	7.183	0.632	1.583	13	1.143	2.865	11.37	7.012	0.617	1.621	11	0.967	2.544
9	05480993	1.66	0.00	0.00	NA	0	0.00	NA	1.66	0.000	0.000	NA	0	0.000	NA
10	05481510	23.27	13.217	0.568	1.761	17	0.730	2.265	23.27	10.852	0.466	2.145	9	0.387	1.779
11	05481528	0.27	1.632	6.053	0.165	7	25.961	0.708	0.27	1.630	6.044	0.165	7	25.961	0.711
12	05481680	40.27	40.049	0.995	1.006	85	2.111	2.134	40.27	34.564	0.858	1.165	58	1.440	1.955
13	05481690	14.76	24.960	1.691	0.591	53	3.592	1.255	14.76	21.986	1.490	0.671	37	2.507	1.129
14	05482600	41.99	44.255	1.054	0.949	97	2.310	2.080	41.99	38.072	0.907	1.103	69	1.643	1.999
15	05482800	8.66	2.078	0.240	4.169	2	0.231	4.013	8.66	2.012	0.232	4.306	1	0.115	2.140
16	05483000	23.31	6.482	0.278	3.596	11	0.472	6.102	23.31	6.316	0.271	3.690	8	0.343	4.675
17	06604584	4.04	3.584	0.888	1.127	6	1.486	1.886	4.04	3.057	0.757	1.321	5	1.238	2.160
		[2]0.0083	1.0000	0.8176	0.8536	[2]0.0007	0.0002	0.0001	[2]0.0083	0.7119	0.3060	0.4307	[2]0.0012	0.0005	0.0006
		88.2	100.0	100.0	100.0	94.1	100.0	100.0	88.2	100.0	100.0	100.0	94.1	100.0	100.0

[1] In general, p-values greater than 0.05 indicate that there is not a statistically significant difference between the median of the StreamStats measurements and the median of the lidar measurements, using a 95-percent level of significance for a two-tailed Wilcoxon signed-rank test.

[2] Using Wilcoxon signed-rank test with continuity correction, which is an adjustment that is made when a discrete distribution is approximated by a continuous distribution, cannot compute exact p-value.

Development of Regional Peak-Flow Regression Equations using Lidar Basin Characteristics

The combination of five different stream initiation methods (NHD; IDNR; and minimum profile curvature thresholds of 0.5, 1.0, and 1.75) and three different watershed delineations (total, 2 percent, and 20 percent) for each of the 17 streamgages created 15 different datasets of selected basin-characteristic values. Each dataset comprised 58 basin-characteristic values for each of the 17 streamgages, with the exception of streamgage 05480993.

Development of Regression Models

Regression analyses were done for each of the 15 datasets to develop the best regression model for each dataset on the basis of a single selected AEPD. The AEPs of 4, 2, and 1 percent, or flood recurrence intervals of 25, 50, and 100 years, were selected for the development of regression equations for this study, because these AEPs are those used most frequently by Iowa Department of Transportation (DOT) for flood estimation (Eash, 2015). Regression models developed for the total watershed delineations were optimized using the 1-percent AEPD, regression models developed for the 2-percent watershed delineations were optimized using the 2-percent AEPD, and regression models developed for the 20-percent watershed delineations were optimized using the 4-percent AEPD.

The same basin characteristics or explanatory variables determined to be the most significant for the development of the best regression model for each dataset based on a single selected AEP also were used for the development of regression equations for the other seven AEPs. Thus, regression equations developed for each of the eight AEPs include the same explanatory variables to minimize the possibility of predictive inconsistencies between estimates of different AEPs. This had previously been done for the development of peak-flow regression equations for Iowa by Eash and others (2013, tables 9–11), when the 1-percent AEP was used to optimize the development of RREs. Predictive inconsistencies result when the discharge estimate for a larger probability is greater than the discharge estimate for a smaller probability; for example, when a 2-percent AEPD estimate is greater than a 1-percent AEPD estimate.

Determination of Predictive Accuracy

Comparisons for the 15 regression datasets were evaluated 2 different ways to determine which of the 5 stream initiation methods provides the most accurate results for each of the 3 watershed delineations and to determine if the combination of a specific stream initiation method and watershed delineation method would provide the best overall predictive accuracy. First, the stream initiation method that provides the best mean predictive accuracy for the three AEPs used most frequently by Iowa DOT (4, 2, and 1 percent) was determined. Second, the stream initiation method that provides the best mean predictive accuracy for all eight AEPs also was determined.

Generalized least-squares (GLS) multiple-linear regression analyses were done by using the weighted-multiple-linear-regression program (Eng and others, 2009) for the development of RREs to estimate AEPDs for the Des Moines Lobe landform region. The GLS multiple-linear regression analyses were weighted on the basis of streamgage record length and on the variance and cross correlation of the annual peak discharges. Cross correlation accounts for the correlation of concurrent streamflow in the time series of each pair of streamgages in a region (Eng and others, 2009), and less weight is factored for streamgages that have greater cross correlation as part of the overall weighting used in GLS regression. The pseudo-R^2, or pseudo coefficient of determination, is a measure of the percentage of the variation explained by the basin characteristics (explanatory variables) included in the model. The pseudo-R^2 value is calculated on the basis of the degrees of freedom in the regression (Griffis and Stedinger, 2007). Final GLS regression models were selected primarily on the basis of minimizing values of the standard error of model (SEM) and the average standard error of prediction (SEP) and maximizing values of the pseudo-R^2. Multicollinearity was explored with the use of the statistical software package R (R Development Core Team, 2016) by checking each explanatory variable for a variance inflation factor greater than two.

StreamStats Regression Equations

To provide a baseline for evaluating the predictive accuracy of RREs developed in this study using lidar basin characteristics, RREs for the Des Moines Lobe landform region also were developed using basin characteristics measured from StreamStats data for the same 17 streamgages. The StreamStats basin characteristics were measured using 1:24,000-scale topographic-map data from stream networks, basin boundaries, and 10-m DEMs (Eash and others, 2013).

For the 17 streamgages included in this study (table 1), the best GLS regression model developed for the 1-percent AEP and then used for the other 7 AEPs, using StreamStats basin characteristics, was a single-variable model. The single-variable RREs developed for this study using StreamStats basin characteristics (table 4) require only DRNAREA, which are comparable to total watershed delineations from the lidar DEMs. Whereas a three-variable model was developed for the Des Moines Lobe landform region for flood region 1 using StreamStats basin characteristics in the most recent study (Eash and others, 2013), only single-variable models requiring drainage-area measurements were developed for the Des Moines Lobe landform region in previous studies (Lara, 1973, 1987; Eash, 2001).

For the StreamStats RREs developed using the 17 streamgages, SEPs range from 55.0 to 74.7 percent, with a mean SEP for $Q_{4\%}$, $Q_{2\%}$, and $Q_{1\%}$ (Q values are the AEPDs for the indicated flood-discharge recurrence interval) of 57.0 percent and a mean SEP for all 8 AEPs of 60.8 percent (table 4). For comparison, StreamStats RREs developed using 91 streamgages in flood region 1 have SEPs that range from 31.8 to 45.2 percent for multivariable equations (table 9 in Eash and others, 2013) and from 42.4 to 55.8 percent for single-variable equations (table 5 in Eash, 2015). The single-variable equations (table 5 in Eash, 2015) have a mean SEP for $Q_{4\%}$, $Q_{2\%}$, and $Q_{1\%}$ of 46.6 percent and a mean SEP for all eight AEPs of 48.1 percent. The better predictive accuracies obtained for the single-variable RREs developed using 91 streamgages (table 5 in Eash, 2015), compared to those developed in this study using 17 streamgages (table 4), indicates less overall variation in peak discharges for the 91 streamgages compared to peak discharges for the 17 streamgages. The natural variability of peak discharges may be an important factor associated with the predictive accuracy of AEPDs. Estimation of AEPDs that have greater variability will have poorer predictive accuracies than estimation of AEPDs with less variability.

Lidar Regression Equations

Results of the regression analyses of the 15 lidar datasets for selected stream-initiation methods and selected watershed delineation methods are listed in table 5. The table lists the most significant basin characteristics used to develop the best regression model for each dataset, three performance metrics, and the number of streamgages included in each regression analysis. All basin characteristics included in the regression results (table 5) were statistically significant at the 95-percent confidence level, and they were not correlated with basin characteristics used in the same equation. The performance metrics in table 5 indicate the predictive accuracy of the RREs. A description of the performance metrics reported for the GLS regressions is presented in Eash and others (2013). For streamgage 05480993, no streams are available for the profile curvature stream initiation methods of 1.0 and 1.75, thus complete sets of basin characteristics could be measured only for 16 streamgages for these 2 stream initiation methods.

The mean SEP for $Q_{4\%}$, $Q_{2\%}$, and $Q_{1\%}$ and the mean SEP for all 8 AEPs are used in this study to evaluate the overall predictive accuracy of the RREs developed for each of the 15 datasets. The lowest mean SEPs indicate the best predictive accuracy. For the five stream-initiation methods tested for the total watershed delineations, the NHD, IDNR, and profile curvature of 0.5 stream-initiation methods produced the lowest mean SEP for $Q_{4\%}$, $Q_{2\%}$, and $Q_{1\%}$ of 57.9 percent, and these same three stream-initiation methods also produced the lowest mean SEP for all eight AEPs of 60.3 percent (table 5). These mean SEP values produced for the total watershed delineations (table 5) indicate a slightly poorer predictive accuracy for the mean of $Q_{4\%}$, $Q_{2\%}$, and $Q_{1\%}$ and a slightly better predictive accuracy for the mean of all eight AEPs when compared to those produced for the RREs developed using the StreamStats data (table 4).

For the five stream-initiation methods tested for the effective watershed delineations for a 2-percent AEP 12-hour rainfall, the NHD, IDNR, and profile curvature of 0.5 stream-initiation methods produced the lowest mean SEP for $Q_{4\%}$, $Q_{2\%}$, and $Q_{1\%}$ of 55.4 percent. The same three stream-initiation methods produced the lowest mean SEP for all eight AEPs of 57.6 percent (table 5). The mean SEP values produced by these three methods using the 2-percent watershed delineations (table 5) indicate a higher predictive accuracy for both the mean of $Q_{4\%}$, $Q_{2\%}$, and $Q_{1\%}$ and the mean of all eight AEPs when compared to those produced for the RREs developed using the StreamStats data (table 4).

For the five stream-initiation methods tested for the effective watershed delineations for a 20-percent AEP 12-hour rainfall, the NHD, IDNR, and profile curvature of 0.5 stream-initiation methods produced the lowest mean SEP for $Q_{4\%}$, $Q_{2\%}$, and $Q_{1\%}$ of 53.9 percent. The same three stream-initiation methods produced the lowest mean SEP for all eight AEPs of 55.5 percent (table 5). These mean SEP values produced for the 20-percent effective watershed delineations (table 5) indicate better predictive accuracy for both the mean of $Q_{4\%}$, $Q_{2\%}$, and $Q_{1\%}$ and the mean of all eight AEPs when compared to those produced for the RREs developed using the StreamStats data (table 4).

Results of the regression analyses of the 15 lidar datasets indicate that the method that produces RREs with the best overall predictive accuracy are the NHD, IDNR, and profile curvature of 0.5 stream-initiation method combined with the 20-percent AEP 12-hour rainfall watershed delineation method, with a mean SEP for $Q_{4\%}$, $Q_{2\%}$, and $Q_{1\%}$ of 53.9 percent and a mean SEP for all 8 AEPs of 55.5 percent (table 6). Compared to the RREs developed in this study using

Table 4. Regression equations developed using StreamStats basin characteristics for estimating annual exceedance-probability discharges for unregulated streams in the Des Moines Lobe landform region in Iowa with drainage areas less than 50 square miles.

[AEP, annual exceedance probability; SEP, average standard error of prediction; Pseudo-R^2, pseudo coefficient of determination; SEM, average standard error of model; $Q_{x\%}$, annual exceedance probability discharge of x percent; DRNAREA, geographic-information-system drainage area]

AEP equation	SEP (percent)[1]	Pseudo-R^2 (percent)	SEM (percent)
(17 streamgages used to develop equations)			
$Q_{50\%}$ = 46.2 DRNAREA$^{0.551}$	74.7	59.6	68.1
$Q_{20\%}$ = 123 DRNAREA$^{0.494}$	58.5	63.3	52.9
$Q_{10\%}$ = 194 DRNAREA$^{0.468}$	55.0	62.7	49.2
$Q_{4\%}$ = 308 DRNAREA$^{0.439}$	55.0	58.8	48.6
$Q_{2\%}$ = 407 DRNAREA$^{0.419}$	56.8	54.5	49.8
$Q_{1\%}$ = 520 DRNAREA$^{0.401}$	59.1	49.8	51.6
$Q_{0.5\%}$ = 644 DRNAREA$^{0.384}$	61.8	45.1	53.7
$Q_{0.2\%}$ = 822 DRNAREA$^{0.365}$	65.3	39.2	56.6

[1]Mean SEP for $Q_{4\%}$, $Q_{2\%}$, and $Q_{1\%}$ = 57.0 percent; mean SEP for all eight AEPs = 60.8 percent.

Table 5. Results of the regression analyses of lidar datasets for selected stream-initiation methods and selected watershed delineation methods.

[NHD, National Hydrography Dataset; IDNR, Iowa Department of Natural Resources; CRV 0.5, channel-profile curvature of 0.5 percent; AEP, annual exceedance probability; SEP, average standard error of prediction; Pseudo-R^2, pseudo coeffcient of determination, SEM, average standard error of model; $Q_{x\%}$, annual exceedance probability discharge of x percent; DRNAREA, geographic-information-system drainage area; CRV 1.0, channel-profile curvature of 1.0 percent; CRV 1.75, channel-profile curvature of 1.75 percent]

Results for the following lidar datasets:
1) NHD stream network and total watershed delineation
2) IDNR stream network and total watershed delineation
3) CRV 0.5 Stream network and total watershed delineation

AEP	Most significant basin characteristic	SEP (percent)[1]	Pseudo-R^2 (percent)	SEM (percent)
(17 streamgages used to develop equations)				
$Q_{50\%}$	DRNAREA	74.8	59.8	68.1
$Q_{20\%}$	DRNAREA	60.0	62.2	54.3
$Q_{10\%}$	DRNAREA	57.4	60.2	51.7
$Q_{4\%}$	DRNAREA	57.2	55.9	51.0
$Q_{2\%}$	DRNAREA	58.0	51.8	51.2
$Q_{1\%}$	DRNAREA	58.5	47.8	51.2
$Q_{0.5\%}$	DRNAREA	58.5	44.4	50.6
$Q_{0.2\%}$	DRNAREA	57.9	39.9	49.1

[1]Mean SEP for $Q_{4\%}$, $Q_{2\%}$, and $Q_{1\%}$ = 57.9 percent; mean SEP for all eight AEPs = 60.3 percent.

Results for the following lidar datasets:
1) CRV 1.0 stream network and total watershed delineation
2) CRV 1.75 stream network and total watershed delineation

AEP	Most significant basin characteristic	SEP (percent)[1]	Pseudo-R^2 (percent)	SEM (percent)
(16 streamgages used to develop equations)				
$Q_{50\%}$	DRNAREA	77.2	60.4	70.0
$Q_{20\%}$	DRNAREA	62.0	62.5	56.0
$Q_{10\%}$	DRNAREA	59.8	60.1	53.6
$Q_{4\%}$	DRNAREA	60.0	55.1	53.4
$Q_{2\%}$	DRNAREA	61.0	50.9	53.8
$Q_{1\%}$	DRNAREA	61.8	46.7	53.9
$Q_{0.5\%}$	DRNAREA	62.2	42.9	53.7
$Q_{0.2\%}$	DRNAREA	61.9	38.1	52.5

[1]Mean SEP for $Q_{4\%}$, $Q_{2\%}$, and $Q_{1\%}$ = 60.9 percent; mean SEP for all eight AEPs = 63.2 percent.

Results for the following lidar datasets:
1) NHD stream network and an effective watershed delineation for a 2-percent AEP 12-hour rainfall
2) IDNR stream network and an effective watershed delineation for a 2-percent AEP 12-hour rainfall
3) CRV 0.5 Stream network and an effective watershed delineation for a 2-percent AEP 12-hour rainfall

AEP	Most significant basin characteristic	SEP (percent)[1]	Pseudo-R^2 (percent)	SEM (percent)
(17 streamgages used to develop equations)				
$Q_{50\%}$	DRNAREA	71.4	62.8	65.0
$Q_{20\%}$	DRNAREA	56.8	65.7	51.4
$Q_{10\%}$	DRNAREA	54.5	63.9	49.0
$Q_{4\%}$	DRNAREA	54.6	59.5	48.6
$Q_{2\%}$	DRNAREA	55.5	55.6	48.9
$Q_{1\%}$	DRNAREA	56.2	51.6	49.1
$Q_{0.5\%}$	DRNAREA	56.4	48.3	48.6
$Q_{0.2\%}$	DRNAREA	55.7	44.4	47.0

[1]Mean SEP for $Q_{4\%}$, $Q_{2\%}$, and $Q_{1\%}$ = 55.4 percent; mean SEP for all eight AEPs = 57.6 percent.

Table 5. Results of the regression analyses of lidar datasets for selected stream-initiation methods and selected watershed delineation methods.—Continued

[NHD, National Hydrography Dataset; IDNR, Iowa Department of Natural Resources; CRV 0.5, channel-profile curvature of 0.5 percent; AEP, annual exceedance probability; SEP, average standard error of prediction; Pseudo-R^2, pseudo coeffcient of determination, SEM, average standard error of model; $Q_{x\%}$, annual exceedance probability discharge of x percent; DRNAREA, geographic-information-system drainage area; CRV 1.0, channel-profile curvature of 1.0 percent; CRV 1.75, channel-profile curvature of 1.75 percent]

Results for the following lidar datasets:
1) CRV 1.0 stream network and an effective watershed delineation for a 2-percent AEP 12-hour rainfall
2) CRV 1.75 stream network and an effective watershed delineation for a 2-percent AEP 12-hour rainfal

AEP	Most significant basin characteristic	SEP (percent)[1]	Pseudo-R^2 (percent)	SEM (percent)
(16 streamgages used to develop equations)				
$Q_{50\%}$	DRNAREA	73.7	63.3	66.8
$Q_{20\%}$	DRNAREA	58.9	65.8	53.1
$Q_{10\%}$	DRNAREA	56.9	63.5	51.0
$Q_{4\%}$	DRNAREA	57.4	58.7	50.9
$Q_{2\%}$	DRNAREA	58.5	54.7	51.4
$Q_{1\%}$	DRNAREA	59.4	50.5	51.8
$Q_{0.5\%}$	DRNAREA	60.0	46.6	51.7
$Q_{0.2\%}$	DRNAREA	59.7	42.4	50.4

[1]Mean SEP for $Q_{4\%}$, $Q_{2\%}$, and $Q_{1\%}$ = 58.4 percent; mean SEP for all eight AEPs = 60.6 percent.

Results for the following lidar datasets:
1) NHD stream network and an effective watershed delineation for a 20-percent AEP 12-hour rainfall
2) IDNR stream network and an effective watershed delineation for a 20-percent AEP 12-hour rainfall
3) CRV 0.5 Stream network and an effective watershed delineation for a 20-percent AEP 12-hour rainfall

AEP	Most significant basin characteristic	SEP (percent)[1]	Pseudo-R^2 (percent)	SEM (percent)
(17 streamgages used to develop equations)				
$Q_{50\%}$	DRNAREA	66.6	67.0	60.5
$Q_{20\%}$	DRNAREA	53.3	69.6	48.1
$Q_{10\%}$	DRNAREA	51.9	67.0	46.6
$Q_{4\%}$	DRNAREA	52.8	62.0	46.9
$Q_{2\%}$	DRNAREA	54.1	57.7	47.6
$Q_{1\%}$	DRNAREA	54.9	53.8	47.8
$Q_{0.5\%}$	DRNAREA	55.4	50.0	47.7
$Q_{0.2\%}$	DRNAREA	54.9	46.0	46.3

[1]Mean SEP for $Q_{4\%}$, $Q_{2\%}$, and $Q_{1\%}$ = 53.9 percent; mean SEP for all eight AEPs = 55.5 percent.

Results for the following lidar datasets:
1) CRV 1.0 stream network and an effective watershed delineation for a 20-percent AEP 12-hour rainfall
2) CRV 1.75 stream network and an effective watershed delineation for a 20-percent AEP 12-hour rainfall

AEP	Most significant basin characteristic	SEP (percent)[1]	Pseudo-R^2 (percent)	SEM (percent)
(16 streamgages used to develop equations)				
$Q_{50\%}$	DRNAREA	68.9	67.3	62.4
$Q_{20\%}$	DRNAREA	55.4	69.4	49.9
$Q_{10\%}$	DRNAREA	54.2	66.7	48.5
$Q_{4\%}$	DRNAREA	55.5	61.2	49.2
$Q_{2\%}$	DRNAREA	57.0	56.7	50.1
$Q_{1\%}$	DRNAREA	58.2	52.4	50.7
$Q_{0.5\%}$	DRNAREA	59.0	48.3	50.7
$Q_{0.2\%}$	DRNAREA	58.9	44.0	49.6

[1]Mean SEP for $Q_{4\%}$, $Q_{2\%}$, and $Q_{1\%}$ = 56.9 percent; mean SEP for all eight AEPs = 58.4 percent.

the StreamStats basin characteristics (table 4), the lidar basin characteristics (table 6) provide better overall predictive accuracy. Because only a single-variable model could be developed for each of the 15 datasets and the values for DRNAREA are identical for each of the 5 stream initiation methods within a watershed delineation method, the SEP values are the same for the NHD, IDNR, and profile curvature of 0.5 stream-initiation methods with datasets of 17 streamgages. The SEP values are also the same for the profile curvatures of 1.0 and 1.75 stream initiation methods with datasets of 16 streamgages. The 3 datasets within each watershed delineation method with 17 streamgages have slightly lower SEPs compared to the 2 datasets with 16 streamgages (table 5).

Accuracy and Limitations of Regression Equations

The RREs based on lidar-derived data (or lidar RREs) that were developed in this study apply only to stream sites in the Des Moines Lobe landform region where peak discharges are not affected significantly by regulation, diversion, channelization, backwater, or urbanization. The applicability and accuracy of the lidar RREs depend on whether the basin characteristics measured for an ungaged stream site are within the range of the characteristic values used to develop the RREs. The acceptable range of basin-characteristic values used to develop each lidar RRE (table 6) are tabulated as minimum and maximum values in table 7. The applicability of the RREs is unknown when any characteristic value measured for an ungaged site is outside the studied range. In addition, basin-characteristic measurements at ungaged sites should be computed using the same GIS datasets and measurement methods used in this study. GIS software is required to measure the basin characteristics included as explanatory variables in table 6.

The AEPD regression equations presented in this report should be used with caution for ungaged stream sites for which basin-characteristic values approach the minimum or maximum limits (table 7), because the predictive errors of the equations increase with distance from the mean or median values of the explanatory variables, and thus inconsistencies in the estimates may result. For different AEPs, the AEPD estimate for a larger probability may be greater than the AEPD estimate for a smaller probability; for example, a $Q_{2\%}$ flood discharge estimate may be greater than a $Q_{1\%}$ flood discharge estimate. Although no inconsistencies in RRE estimates resulted for any of the 8 AEPDs for the 17 streamgages listed in table 1, it is possible that inconsistencies in RRE estimates may result for ungaged sites. If inconsistencies in RRE estimates are obtained for an ungaged stream site, a comparison of all AEPDs for the site and a check of streamgage data or other published data may help to determine which AEPD is inconsistent.

In general, predictive accuracies for the best lidar regression equations (table 6) are best for $Q_{10\%}$ and poorest for $Q_{50\%}$. For the best lidar regression equations, SEPs range from 51.9 to 66.6 percent (table 6). In the response variables explained by the explanatory variables (pseudo-R^2) for the best lidar regression equations, the percentages of variation range from 46.0 to 69.6 percent (table 6).

Table 6. Best regression equations developed using lidar basin characteristics for estimating annual exceedance-probability discharges for unregulated streams in the Des Moines Lobe landform region in Iowa with drainage areas less than 50 square miles.

[AEP, annual exceedance probability; SEP, average standard error of prediction; Pseudo-R^2, pseudo coefficient of determination; SEM, average standard error of model; $Q_{x\%}$, annual exceedance probability discharge of x percent; NHD, National Hydrography Dataset; IDNR, Iowa Department of Natural Resources; DRNAREA, geographic-information-system drainage area]

AEP equation	SEP (percent)[1]	Pseudo-R^2 (percent)	SEM (percent)
(17 streamgages used to develop equations using the NHD, IDNR, and profile curvature of 0.5 stream-initiation methods combined with the 20-percent watershed delineation method)			
$Q_{50\%} = 49.0\ \mathrm{DRNAREA}^{0.595}$	66.6	67.0	60.5
$Q_{20\%} = 132\ \mathrm{DRNAREA}^{0.526}$	53.3	69.6	48.1
$Q_{10\%} = 209\ \mathrm{DRNAREA}^{0.490}$	51.9	67.0	46.6
$Q_{4\%} = 331\ \mathrm{DRNAREA}^{0.451}$	52.8	62.0	46.9
$Q_{2\%} = 447\ \mathrm{DRNAREA}^{0.426}$	54.1	57.7	47.6
$Q_{1\%} = 575\ \mathrm{DRNAREA}^{0.404}$	54.9	53.8	47.8
$Q_{0.5\%} = 708\ \mathrm{DRNAREA}^{0.385}$	55.4	50.0	47.7
$Q_{0.2\%} = 912\ \mathrm{DRNAREA}^{0.363}$	54.9	46.0	46.3

[1]Mean SEP for $Q_{4\%}$, $Q_{2\%}$, and $Q_{1\%}$ = 53.9 percent; mean SEP for all eight AEPs = 55.5 percent.

Table 7. Range of lidar basin-characteristic values used to develop the best annual exceedance-probability regression equations for unregulated streams in the Des Moines Lobe landform region in Iowa with drainage areas less than 50 square miles.

[GIS, geographic information system; DRNAREA, drainage area; mi², square miles; lidar, light detection and ranging; NHD, National Hydrography Dataset; IDNR, Iowa Department of Natural Resources]

	GIS DRNAREA (mi^2)
Lidar regression equations were developed using the NHD, IDNR, and profile curvature of 0.5 stream-initiation methods combined with the 20-percent watershed delineation method	
Minimum	0.27
Maximum	37.89
Mean	12.61
Median	6.39
Number of sites	17

Summary

In 2015, the U.S. Geological Survey conducted a study to determine optimum stream-channel delineations from lidar elevation data. The study also was intended to update and improve the predictive accuracy of estimates of annual exceedance-probability discharges (AEPDs) for ungaged stream sites in the Des Moines Lobe landform region. This study investigated five different methods to define stream initiation using 3-meter light detecting and ranging (lidar) digital elevation model (DEM) data for 17 streamgages with drainage areas less than 50 square miles within the Des Moines Lobe landform region in north-central Iowa. The DEMs of watersheds for the 17 streamgages were hydrologically enforced, and the 5 stream initiation methods were used to define channel initiation points and the downstream flow paths. The five stream initiation methods include: (1) streams derived from National Hydrography Dataset (NHD) data, (2) streams derived by the Iowa Department of Natural Resources (IDNR), (3) streams derived from a minimum profile curvature threshold of 0.5, (4) streams derived from a minimum profile curvature threshold of 1.0, and (5) streams derived from a minimum profile curvature threshold of 1.75. The five different methods to define stream initiation were tested side-by-side for three watershed delineations: (1) the total drainage-area delineation, (2) an effective drainage-area delineation of basins based on a 2-percent annual exceedance probability (AEP) 12-hour rainfall, and (3) an effective drainage-area delineation based on a 20-percent AEP 12-hour rainfall.

The AEPDs were estimated for each of the 17 streamgages from observed streamflow data collected through September 30, 2015, using the expected moments algorithm/multiple Grubbs-Beck test streamgage probability-analysis method for AEPs of 50, 20, 10, 4, 2, 1, 0.5, and 0.2 percent. Six basin characteristics measured for the 17 streamgages using lidar data for 3 different stream-initiation methods, and basin characteristics measured for 16 of the streamgages for 2 different stream-initiation methods, were selected to represent measurements of stream-channel length, density, and order. These six selected basin characteristics were used to evaluate which of the five different lidar stream-initiation methods appear to provide stream networks that are most similar to stream networks from StreamStats data. Overall results of the comparison tests appear to indicate that the IDNR lidar stream-initiation method provides stream networks that are most similar to StreamStats stream networks, and the NHD lidar stream-initiation method provides the second most similar. Although the three profile curvature stream initiation methods of 0.5, 1.0, and 1.75 all provide lidar stream networks that are not statistically different from StreamStats stream networks for stream-channel length and stream density, they all are statistically different from StreamStats stream networks for the number of first-order streams and for the related measurements of drainage frequency and relative stream density.

Fifty-eight selected basin-characteristic values were measured for each of the 15 datasets. Regression analyses were done to develop the best regression model for each dataset on the basis of a single selected AEP. AEPs of 4, 2, and 1 percent were selected for the development of regression equations for this study, because these AEPs are used most frequently by Iowa DOT for flood estimation. Comparisons for the 15 regression datasets were evaluated 2 different ways. First, the stream initiation method that provides the best mean predictive accuracy for the three AEPs of 4, 2, and 1 percent was determined. Second, the stream initiation method that provides the best mean predictive accuracy for all eight AEPs also was determined. Generalized least-squares multiple-linear regression analyses were used in the development of regional regression equations (RREs) to estimate AEPDs for the Des Moines Lobe landform region.

To provide a baseline for evaluating the predictive accuracy of RREs developed in this study using lidar basin characteristics, RREs for the Des Moines Lobe landform region also were developed using basin characteristics measured from StreamStats data for the same 17 streamgages. For the StreamStats RREs developed in this study, a mean SEP for $Q_{4\%}$, $Q_{2\%}$, and $Q_{1\%}$ (Q values are the AEPDs for the indicated flood-discharge recurrence interval) of 57.0 percent and a mean SEP for all eight AEPs of 60.8 percent can be compared to the lidar RRE results.

Results for the regression analyses of the 15 lidar datasets indicate the datasets that produce RREs with the best overall predictive accuracy are the NHD, IDNR, and profile curvature of 0.5 stream initiation methods combined with the 20-percent AEP 12-hour rainfall watershed delineations method. The SEP values produced by the RREs for these three specified methods range from 51.9 to 66.6 percent with a mean SEP for $Q_{4\%}$, $Q_{2\%}$, and $Q_{1\%}$ of 53.9 percent and a mean SEP for all eight AEPs of 55.5 percent. For these RREs, the percentages of variation in the response variables explained by the explanatory variables (pseudo-R^2) range from 46.0 to 69.6. These mean SEP values indicate better predictive accuracy for both the mean SEP of $Q_{4\%}$, $Q_{2\%}$, and $Q_{1\%}$ and the mean SEP of all eight AEPs when compared to those produced for the RREs developed using the StreamStats data.

The RREs developed in this study apply only to stream sites in the Des Moines Lobe landform region at which peak discharges are not affected significantly by regulation, diversion, channelization, backwater, or urbanization. The applicability and accuracy of the lidar RREs depend on whether the basin characteristics measured for an ungaged stream site are within the range of the characteristic values used to develop the RREs. Inconsistencies in AEPD estimates may result if basin-characteristic values approach the minimum or maximum limits of the range. Geographic information system software is required to measure the basin characteristics included as explanatory variables in the regression equations.

References Cited

Cohn, T.A., England, J.F., Berenbrock, C.E., Mason, R.R., Stedinger, J.R., and Lamontagne, J.R., 2013, A generalized Grubbs-Beck test statistic for detecting multiple potentially influential low outliers in flood series: Water Resources Research, v. 49, no. 8, p. 5047–5058, accessed July 11, 2016, at https://onlinelibrary.wiley.com/doi/10.1002/wrcr.20392/pdf.

Cohn, T.A., Lane, W.L., and Baier, W.G., 1997, An algorithm for computing moments-based flood quantile estimates when historical flood information is available: Water Resources Research, v. 33, no. 9, p. 2089–2096, accessed July 11, 2016, at https://onlinelibrary.wiley.com/doi/10.1029/97WR01640/pdf.

Cohn, T.A., Lane, W.L., and Stedinger, J.R., 2001, Confidence intervals for Expected Moments Algorithm flood quantile estimates: Water Resources Research, v. 37, no. 6, p. 1695–1706, accessed July 11, 2016, at http://onlinelibrary.wiley.com/doi/10.1029/2001WR900016/pdf.

Colson, T.P., Gregory, J.D., Mitasova, Helena, and Nelson, S.A.C., 2006, Comparison of stream extraction models using lidar DEMs, *in* Geographic Information Systems and Water Resources IV, AWRA Spring Specialty Conference, May 8–10, 2006: Houston, Tex., AWRA Spring Specialty Conference, 7 p., accessed July 11, 2016, at http://www4.ncsu.edu/~hmitaso/gmslab/papers/AWRA2006Tomstreams%20.pdf.

Eash, D.A., 2001, Techniques for estimating flood-frequency discharges for streams in Iowa: U.S. Geological Survey Water-Resources Investigations Report 00–4233, 88 p., accessed July 7, 2016, at https://pubs.er.usgs.gov/publication/wri004233.

Eash, D.A., 2015, Comparisons of estimates of annual exceedance-probability discharges for small drainage basins in Iowa, based on data through water year 2013: U.S. Geological Survey Scientific Investigations Report 2015–5055, 37 p., accessed September 16, 2016, at https://dx.doi.org/10.3133/sir20155055.

Eash, D.A., and Barnes, K.K., 2012, Methods for estimating selected low-flow frequency statistics and harmonic mean flows for streams in Iowa: U.S. Geological Survey Scientific Investigations Report 2012–5171, 99 p., accessed July 7, 2016, at https://pubs.usgs.gov/sir/2012/5171/.

Eash, D.A., Barnes, K.K., and O'Shea, P.S., 2016, Methods for estimating selected spring and fall low-flow frequency statistics for ungaged stream sites in Iowa, based on data through June 2014 (ver. 1.1, October 2016): U.S. Geological Survey Scientific Investigations Report 2016–5111, 32 p., accessed November 18, 2016, at https://doi.org/10.3133/sir20165111.

Eash, D.A., Barnes, K.K., and Veilleux, A. G., 2013, Methods for estimating annual exceedance-probability discharges for streams in Iowa, based on data through water year 2010: U.S. Geological Survey Scientific Investigations Report 2013–5086, 63 p., with appendix, accessed July 7, 2016, at https://pubs.usgs.gov/sir/2013/5086/.

Eng, Ken, Chen, Yin-Yu, and Kiang, J.E., 2009, User's guide to the Weighted-Multiple-Linear-Regression program (WREG version 1.0): U.S. Geological Survey Techniques and Methods, book 4, chap. A8, 21 p., accessed July 7, 2016, at https://pubs.usgs.gov/tm/tm4a8/.

Esri, 2014, ArcGIS Desktop—Release 10.3: Redlands, Calif., Environmental Systems Research Institute.

Gelder, B.K., 2015, Automation of DEM cutting for hydrologic/hydraulic modeling: Institute for Transportation, Iowa State University, 20 p., accessed July 7, 2016, at https://www.intrans.iastate.edu/research/documents/research-reports/DEM_cutting_automation_w_cvr.pdf.

Griffis, V.W., and Stedinger, J.R., 2007, The use of GLS regression in regional hydrologic analyses: Journal of Hydrology, v. 344, p. 82–95, accessed April 11, 2016, at https://doi.org/10.1016/j.jhydrol.2007.06.023.

Heidemann, Hans Karl, 2014, Lidar base specification (ver. 1.2, November 2014): U.S. Geological Survey Techniques and Methods, book 11, chap. B4, 67 p., with appendixes, accessed July 11, 2016, at https://dx.doi.org/10.3133/tm11B4.

Holmes, R.R., Jr.; and Dinicola, Karen, 2010, 100-year flood—It's all about chance: U.S. Geological Survey General Information Product 106, 4 p., accessed July 11, 2016, at https://pubs.usgs.gov/gip/106/pdf/100-year-flood-handout-042610.pdf.

Homer, Collin, Huang, Chengquan, Yang, Limin, Wylie, Bruce, and Coan, Michael, 2004, Development of a 2001 National Land-Cover Database for the United States: Photogrammetric Engineering and Remote Sensing, v. 70, no. 7, p. 829–840, accessed April 7, 2011, at https://www.mrlc.gov/pdf/July_PERS.pdf, also see https://www.mrlc.gov/index.php.

Horton, R.E., 1945, Erosional development of streams and their drainage basins; hydrophysical approach to quantitative morphology: The Geological Society of America Bulletin 56, no. 3, p. 275–370, accessed July 11, 2016, at https://pubs.geoscienceworld.org/gsabulletin/article-abstract/56/3/275/4075/erosional-development-of-streams-and-their?redirectedFrom=fulltext.

Interagency Advisory Committee on Water Data, 1982, Guidelines for determining flood flow frequency: Reston, Va., Hydrology Subcommittee Bulletin 17B, 28 p., plus appendixes, accessed July 7, 2016, at https://water.usgs.gov/osw/bulletin17b/dl_flow.pdf.

James, L.A., and Hunt, K.J., 2010, The lidar-side of headwater streams: mapping channel networks with high-resolution topographic data: Southeastern Geographer, v. 50, no. 4, p. 523–539, accessed July 11, 2016, at http://people.cas.sc.edu/ajames/Research/Pubs/10%20James%20%26%20Hunt%20_LiDAR%20side%20head-wtr%20strms%20_SEG.pdf.

Kaiser, Bill, Ducey, Craig, and Wickwire, Dan, 2010, Evaluation of existing GIS hydrological toolsets for modeling stream networks with lidar and updating the National Hydrography Dataset (NHD): The Oregon LiDAR Hydrography Pilot Project, 27 p., accessed July 11, 2016, at http://www.pnwhf.org/docs/lidar_hydrography_pilotphase_i_final.pdf.

Lara, O.G., 1973, Floods in Iowa—Technical manual for estimating their magnitude and frequency: Iowa Natural Resources Council Bulletin 11, 56 p.

Lara, O.G., 1987, Method for estimating the magnitude and frequency of floods at ungaged sites on unregulated rural streams in Iowa: U.S. Geological Survey Water-Resources Investigations Report 87–4132, 34 p., accessed December 23, 2016, at https://pubs.er.usgs.gov/publication/wri874132.

Linhart, S.M.; Nania, J.F.; Sanders, C.L., Jr.; and Archfield, S.A., 2012, Computing daily mean streamflow at ungaged locations in Iowa by using the Flow Anywhere and Flow Duration Curve Transfer statistical methods: U.S. Geological Survey Scientific Investigations Report 2012–5232, 50 p., accessed July 7, 2016, at https://pubs.usgs.gov/sir/2012/5232/.

Multi-Resolution Land Characteristics Consortium (MRLC), 2011, National Land Cover Database (NLCD): accessed May 2, 2016, at https://www.mrlc.gov/nlcd2011.php.

Oschwald, W.R., Riecken, F.F., Dideriksen, R.I., Scholtes, W.H., and Schaller, F.W., 1965, Principal soils of Iowa: Ames, Iowa State University, Department of Agronomy, Special Report no. 42, 77 p., accessed March 5, 2015, at http://lib.dr.iastate.edu/specialreports/44/.

Perica, Sanja; Martin, Deborah; Pavlovic, Sandra; Roy, Ishani; St. Laurent, Michael; Trypaluk, Carl; Unruh, Dale; Yekta, Michael; Bonnin, Geoffrey, 2013, NOAA Atlas 14—Precipitation-frequency atlas of the United States, volume 8 version 2.0—Midwestern States: Silver Springs, Md., National Oceanic and Atmospheric Administration, National Weather Service, 292 p., accessed July 11, 2016, at http://www.nws.noaa.gov/oh/hdsc/PF_documents/Atlas14_Volume8.pdf.

PRISM Climate Group, 2008, Normal annual precipitation grid for the conterminous United States, accessed January 7, 2016, at http://prism.nacse.org/normals/, also see http://prism.nacse.org/documents/.

Prior, J.C., 1991, Landforms of Iowa: Iowa City, University of Iowa Press, 154 p., accessed July 15, 2016, at http://agronomy.unl.edu/FarmingSystems/organic/resourcevolumes/land-forms-of-iowacari.pdf.

Prior, J.C., Kohrt, C.J., and Quade, D.J., 2009, The landform regions of Iowa, vector digital data: Iowa City, Iowa, Iowa Geological Survey, Iowa Department of Natural Resources, accessed March 9, 2015, at ftp://ftp.igsb.uiowa.edu/gis_library/IA_state/Geologic/Landform/Landform_Regions.html.

R Development Core Team, 2016, R—A language and environment for statistical computing: Vienna, Austria, R Foundation for Statistical Computing, version 3.2.4-revised (2016–0–16): accessed December 20, 2016, at https://www.R-project.org.

Ries, K.G., Guthrie, J.G, Rea, A.H., Steeves, P.A., and Stewart, D.W., 2008, StreamStats—A water resources web application: U.S. Geological Survey Fact Sheet 2008–3067, 6 p. [Also available at https://pubs.usgs.gov/fs/2008/3067/.]

Soil Survey Staff, 2012, Natural Resources Conservation Service, U.S. Department of Agriculture, Web Soil Survey: accessed April 30, 2012, at https://websoilsurvey.sc.egov.usda.gov/.

Strahler, A.N., 1952, Hypsometric (area-altitude) analysis of erosional topology: The Geological Society of America Bulletin 63, no. 11, p. 1117–1142, accessed April 2015, at https://pubs.geoscienceworld.org/gsabulletin/article-abstract/63/11/1117/4477/hypsometric-area-altitude-analysis-of-erosional?redirectedFrom=fulltext.

U.S. Geological Survey, 2016, National Water Information System—Web Interface: U.S. Geological Survey database, accessed April 11, 2016, at https://waterdata.usgs.gov/nwis/sw.

Veilleux, A.G.; Cohn, T.A.; Flynn, K.M.; Mason, R.R., Jr.; and Hummel, P.R., 2014, Estimating magnitude and frequency of floods using the PeakFQ 7.0 program: U.S. Geological Survey Fact Sheet 2013–3108, 2 p., accessed July 7, 2016, at: https://dx.doi.org/10.3133/fs20133108.

Veilleux, A.G., Stedinger, J.R., and Eash, D.A., 2012, Bayesian WLS/GLS regression for regional skewness analysis for regions with large crest stage gage networks, *in* Loucks, E.D., ed., Proceedings of the World Environmental and Water Resources Congress—Crossing boundaries, May 20–24, 2012 [abs.]: Albuquerque, N. Mex., American Society of Civil Engineering, paper 227, p. 2253–2263, accessed July 11, 2016, at https://ia.water.usgs.gov/media/pdf/report/Veilleux-Stedinger-Eash-EWRI-2012-227R.pdf.

Venables, W.N., and Ripley, B.D., 2002, Modern applied statistics with S (4th ed.): New York, Springer, accessed November 30, 2016, at https://www.stats.ox.ac.uk/pub/MASS4/.

For additional information contact:

Director, Central Midwest Water Science Center
U.S. Geological Survey
400 S. Clinton Street
Iowa City, IA 52240

Publishing support provided by the
Madison and Sacramento Publishing Service Centers

Eash and others—**Stream-Channel and Watershed Delineations and Basin-Characteristic Measurements using Lidar Elevation Data**—Scientific Investigations Report 2017–5108

ISSN 2328-0328 (online)
https://doi.org/10.3133/sir200175108